

Dániel Kincses, Márton Nagy, Máté Csanád,

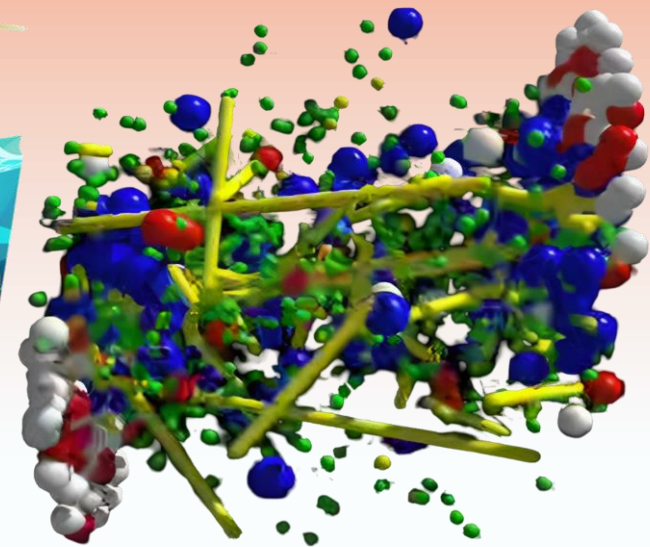
ELTE Eötvös Loránd University, Budapest

Based on

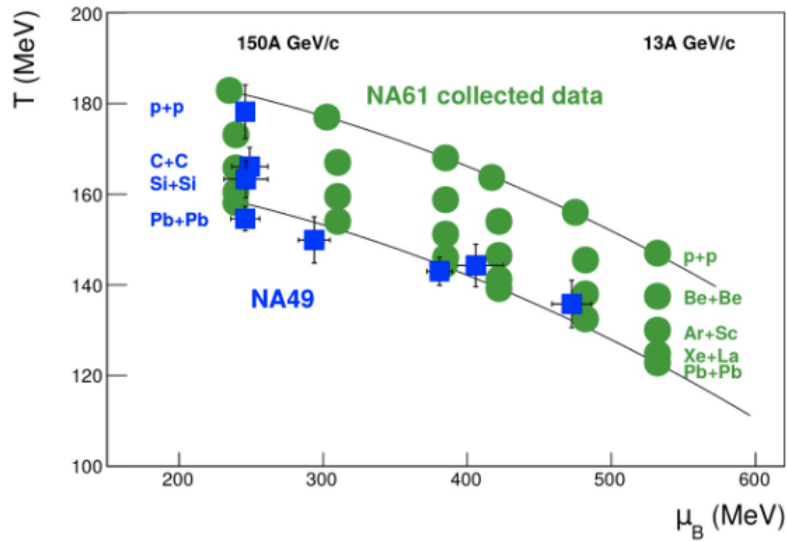
arXiv:2409.10373

**What is common between
marine predators, albatrosses, bacteria,
climate change, and heavy-ion collisions?**

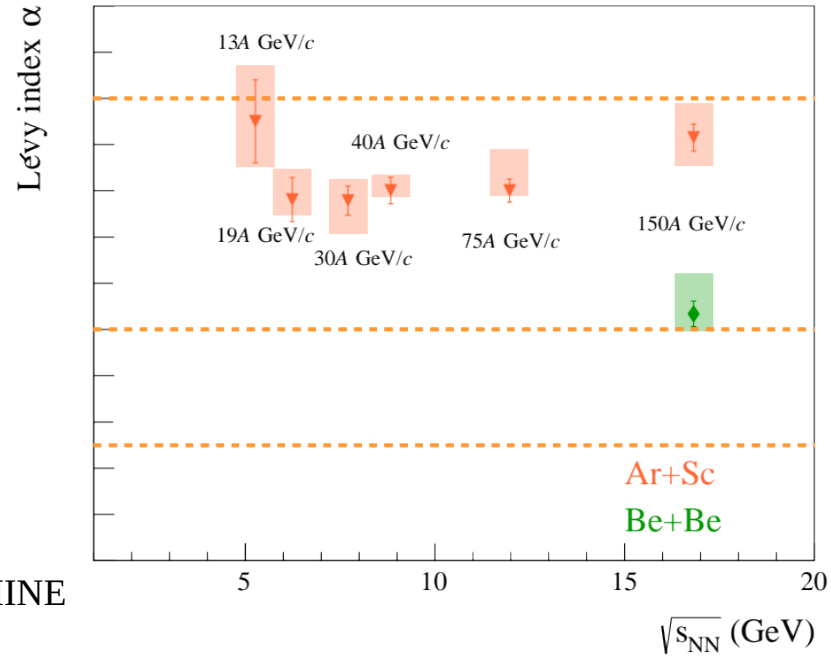
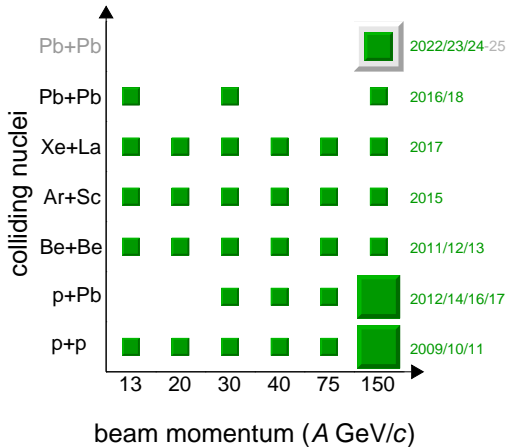
**Check out my poster
and find out!**



Energy scan results with Lévy type femtoscopy at NA61 /SHINE



- Source often assumed to be Gaussian
 - Experimental results show otherwise might bring new, interesting physics
- Is the particle emitting source Gaussian or not?
- Are there signs indicating a critical point?



Energy scan results with Lévy type femtoscopy at NA61 /SHINE

- Source often assumed to be Gaussian
 - Experimental results show otherwise might bring new, interesting physics
- Is the particle emitting source Gaussian or not?
- Are there signs indicating a critical point?

You can find out the answers at my poster!

The aim of the analysis

- Pair source distribution: $D(r, K) = \int S\left(\rho + \frac{r}{2}, K\right) S\left(\rho - \frac{r}{2}, K\right) d^4\rho$
- Shape of the source function?
- Lévy-stable distribution: generalization of Gaussian
- Shown in many experiments: the shape deviates from Gaussian ($\alpha < 2$)

Why?

One possible reason:

Elastic scattering dominated anomalous diffusion:

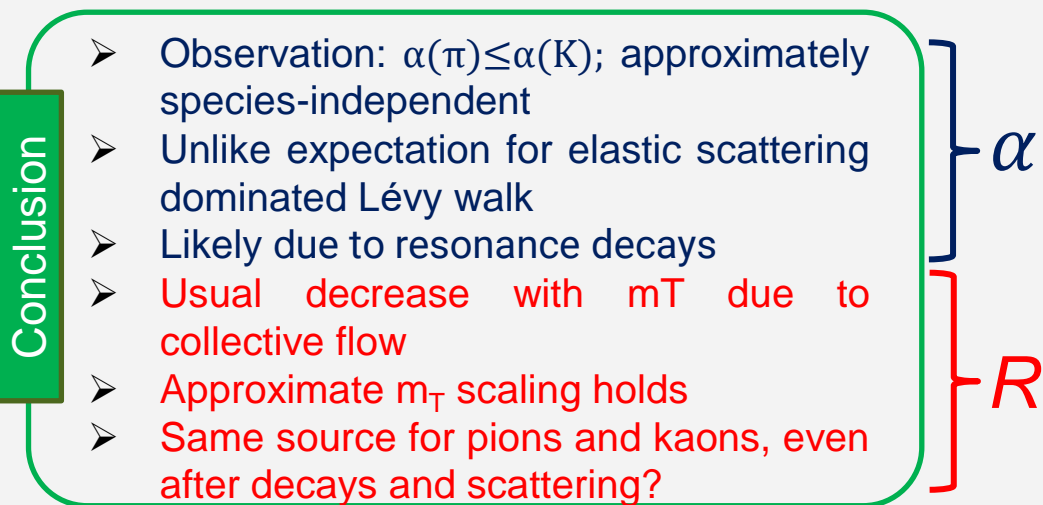
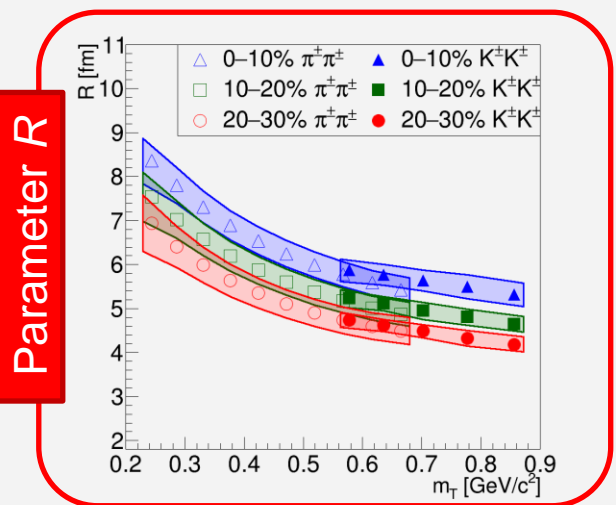
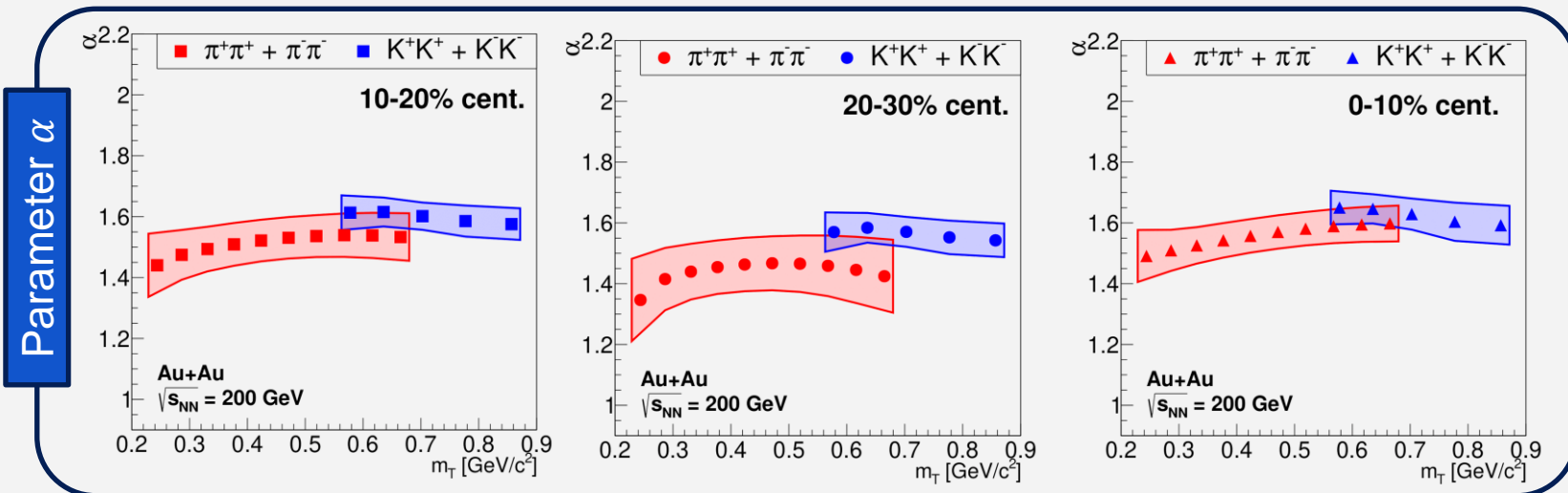


M. Csanád, T. Csörgő, M. Nagy, Braz.J.Phys. 37 (2007) 1002
 Humanic, Int.Jour.Mod.Phys. E 15 (2006) 197

Relation?



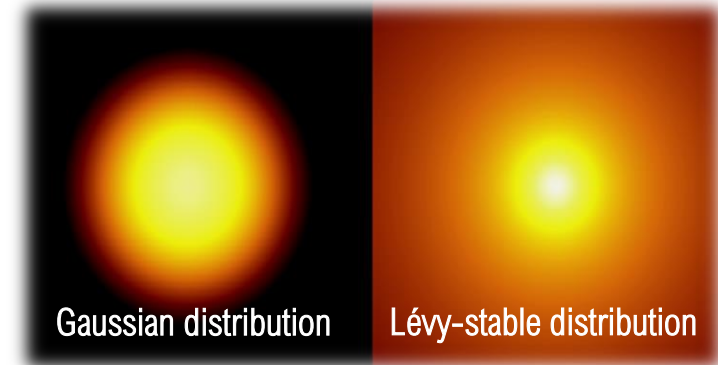
EPOS results



3D pion source images in 200 GeV Au+Au collisions with EPOS

Emese Árpási

Eötvös Loránd University, Budapest



➤ Lévy shape of the pion source function seen in many experiments

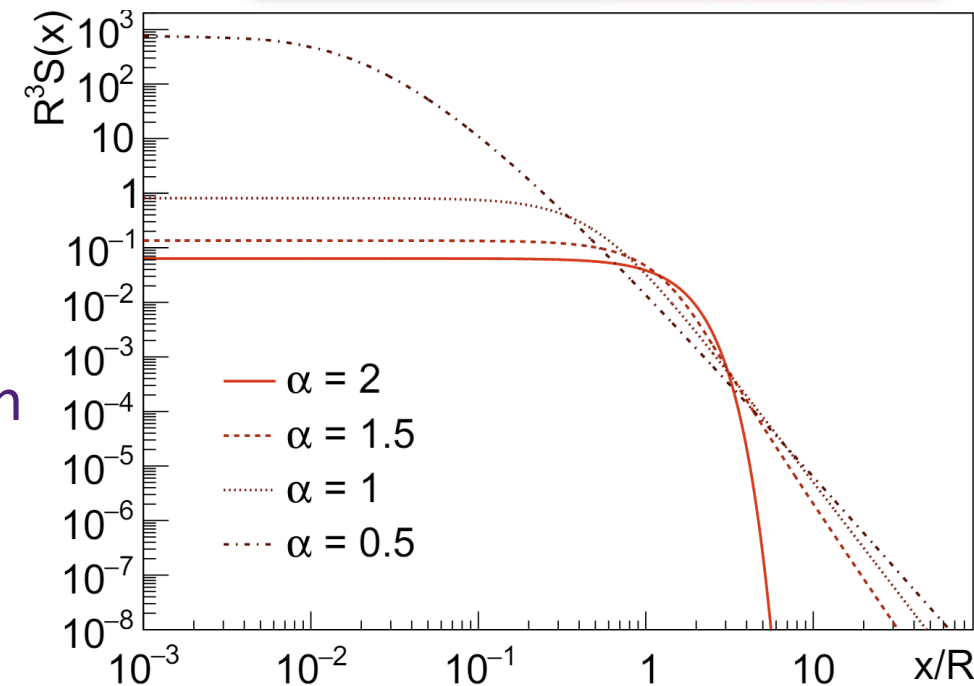
➤ Motivation: does the Lévy shape show up in 3D too?
→ check in EPOS!

➤ $\sqrt{s_{NN}} = 200$ GeV Au+Au collisions generated by the EPOS program package

➤ Event-by-event and 3-dimensional investigation of the pion pair-source

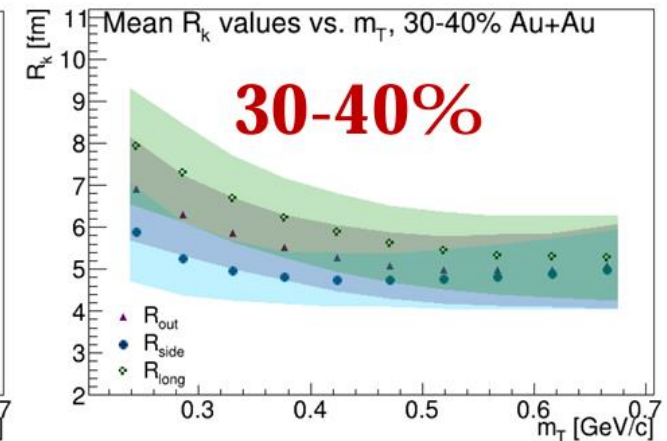
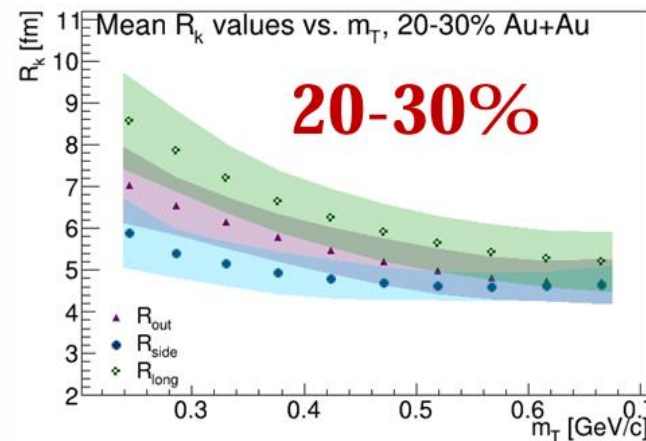
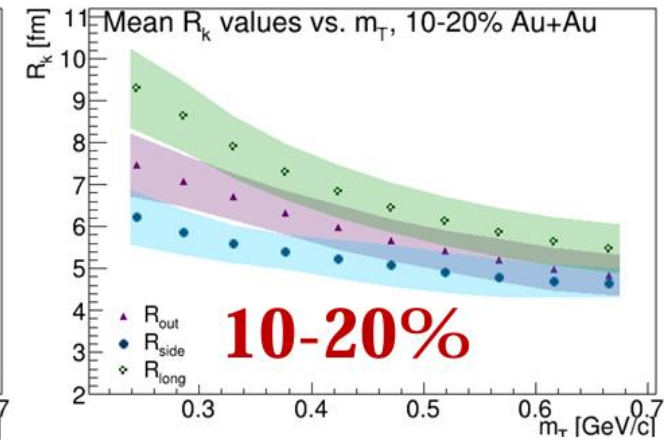
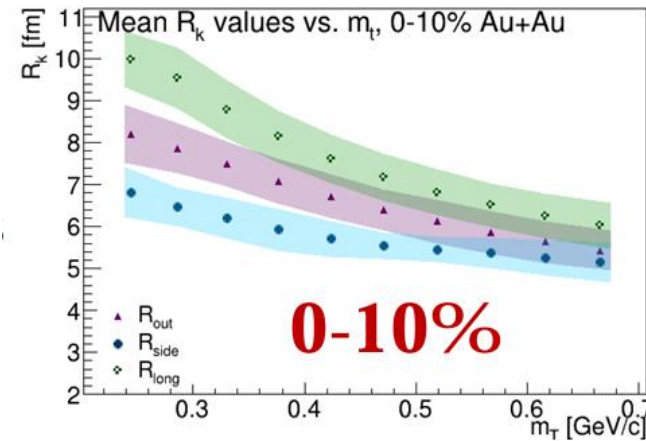
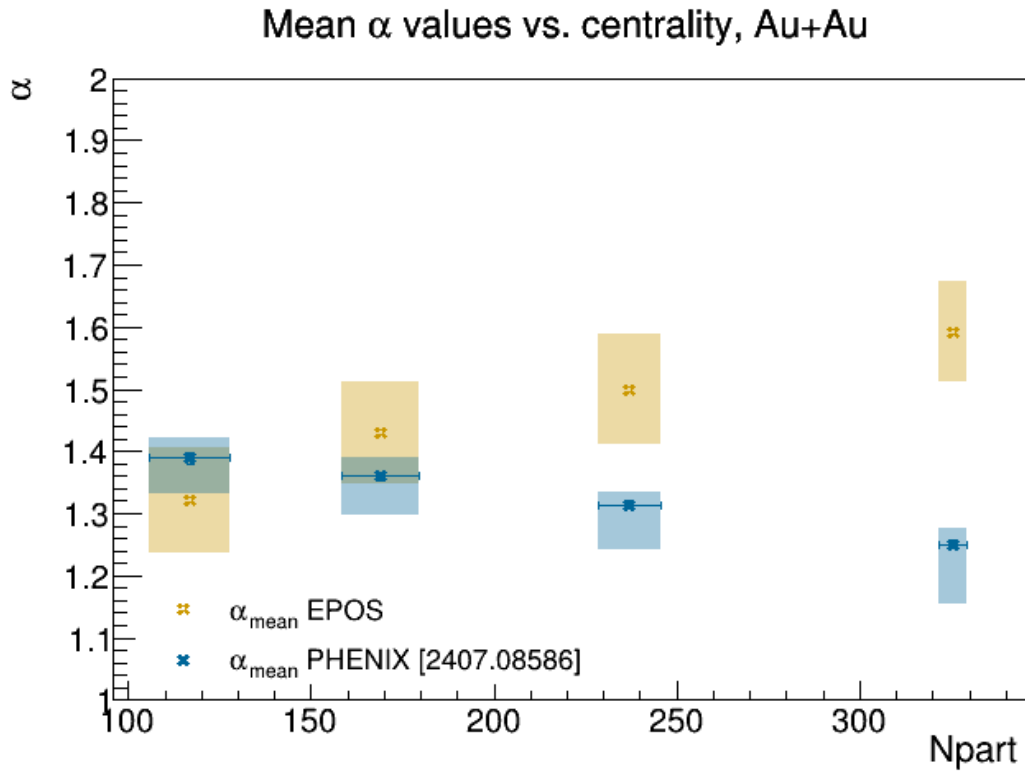
➤ $D(r)$ pion pair source function fitted with Lévy distribution

$$D(r) = \mathcal{L} \left(r, 2^{\frac{1}{\alpha}} R_{out}, 2^{\frac{1}{\alpha}} R_{side}, 2^{\frac{1}{\alpha}} R_{long}, \alpha \right)$$



Results

- Source shape described well by 3D Lévy-stable distributions on an event-by-event basis
- Parameters compared to new final PHENIX angle-averaged results

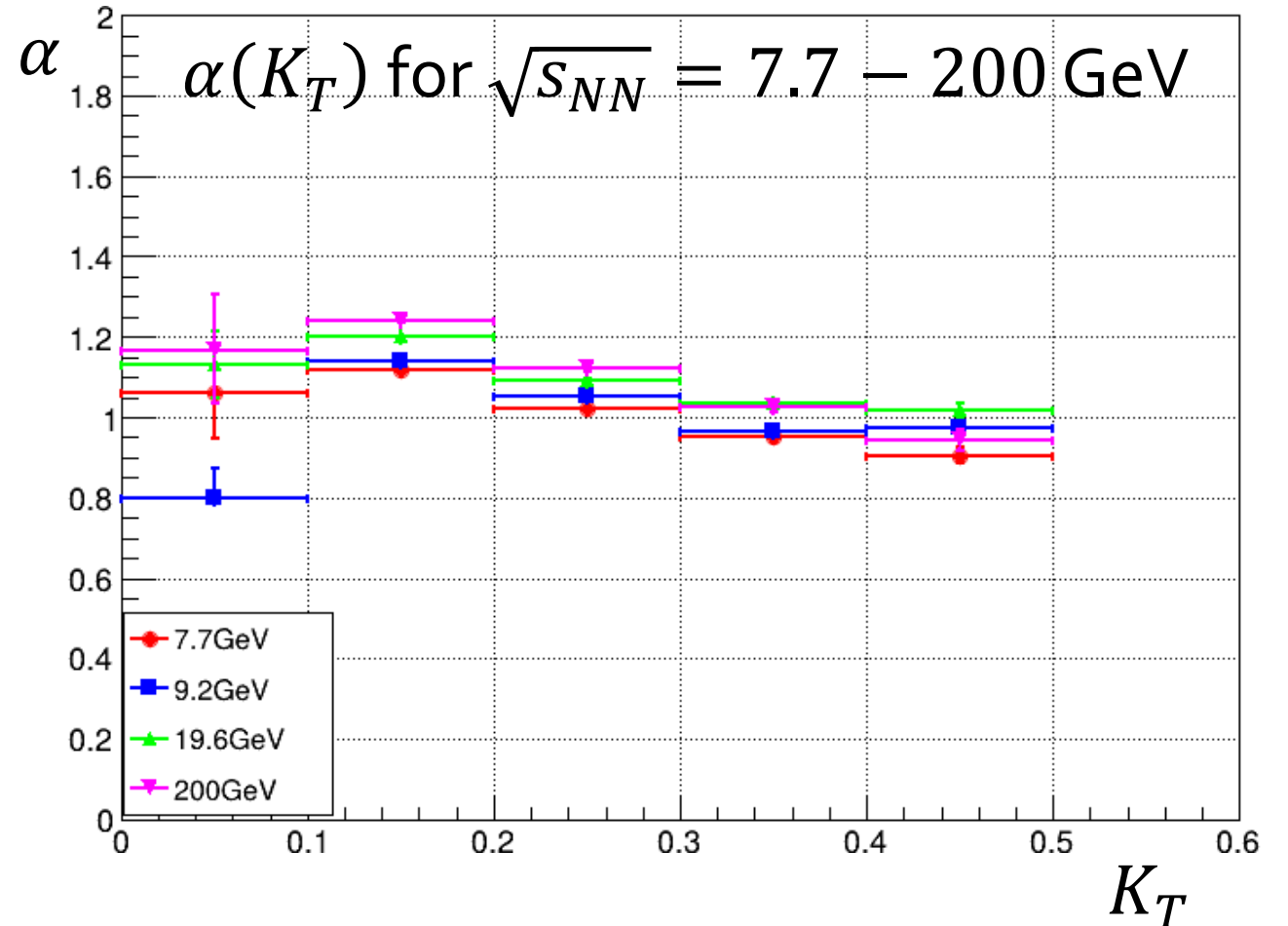
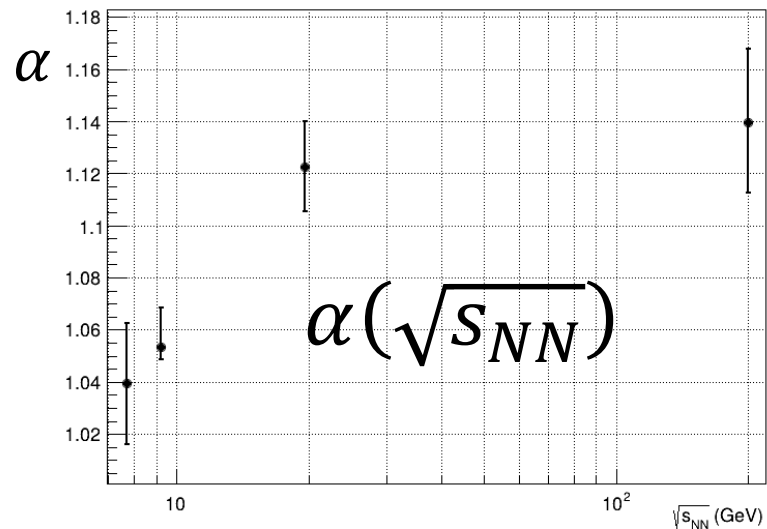


PION EMISSION SOURCE WITH EPOS₄

M. Molnár (Eötvös University)

Shape of pion emission source versus $\sqrt{s_{NN}}$

- Analysis done before in EPOS₃ (see talks by E. Árpási, L. Kovács, D. Kincses, M. Csanád)
- EPOS₄ includes different hadronization
- First preliminary results out: from 7.7 to 200 GeV
 - Slight dependence on K_T
 - To check: fits from event-averaged data
- Collision energy dependence interesting



Elliptic flow of deuterons in heavy-ion collisions

Tomáš Poledníček^a, Boris Tomášik^{a,b}



^aFaculty of Nuclear Sciences and Physical Engineering, Czech Technical University in Prague, Czech Republic

^bUniverzita Mateja Bela, Banská Bystrica, Slovakia



Key Insights and Results

- **Hybrid model:**

- Trento3D - vHLLE - SMASH
- Initial conditions \rightarrow QGP evolution \rightarrow Hadronic phase

- **Tuning of parameters (Trento3D, vHLLE)**

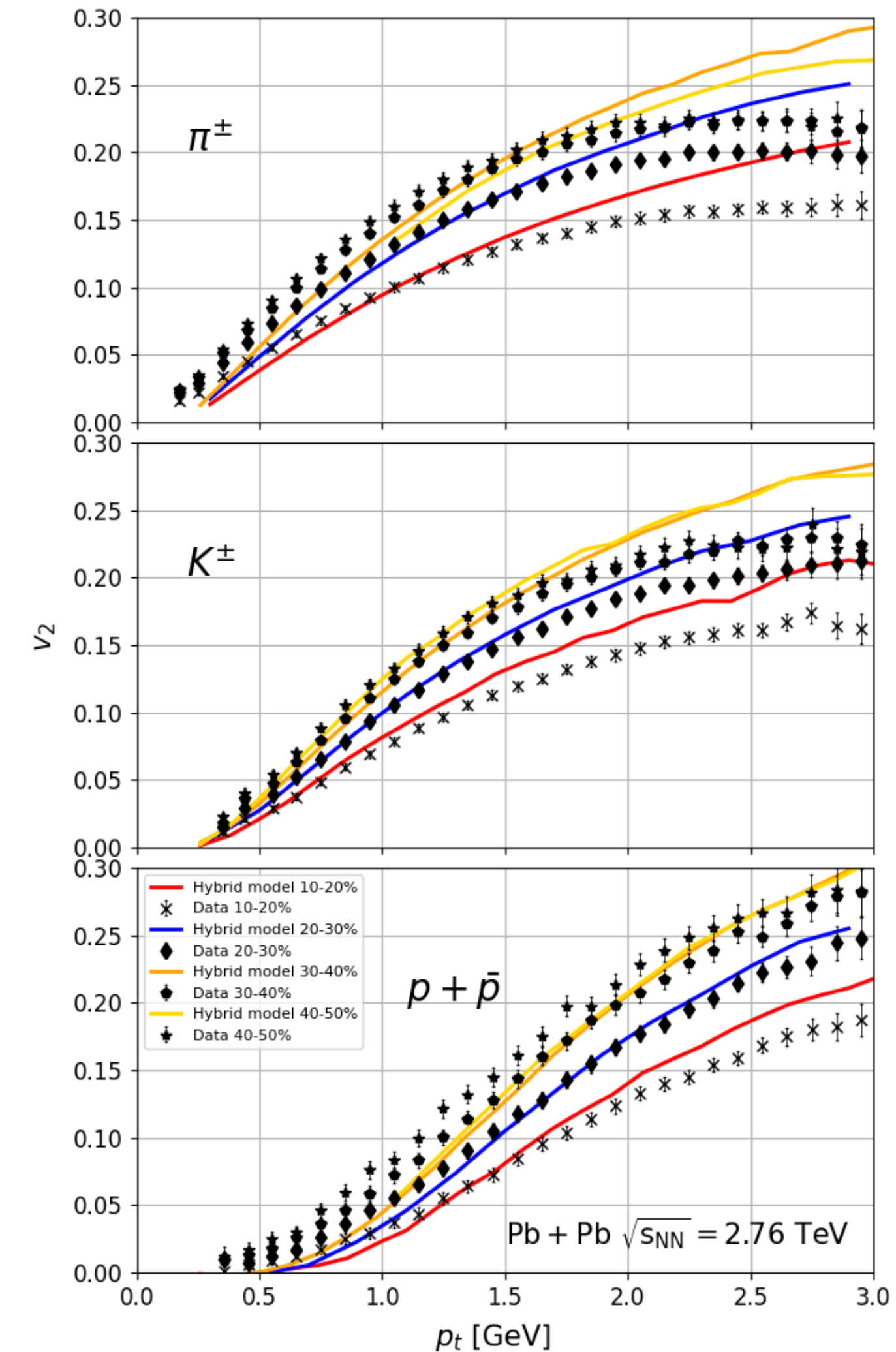
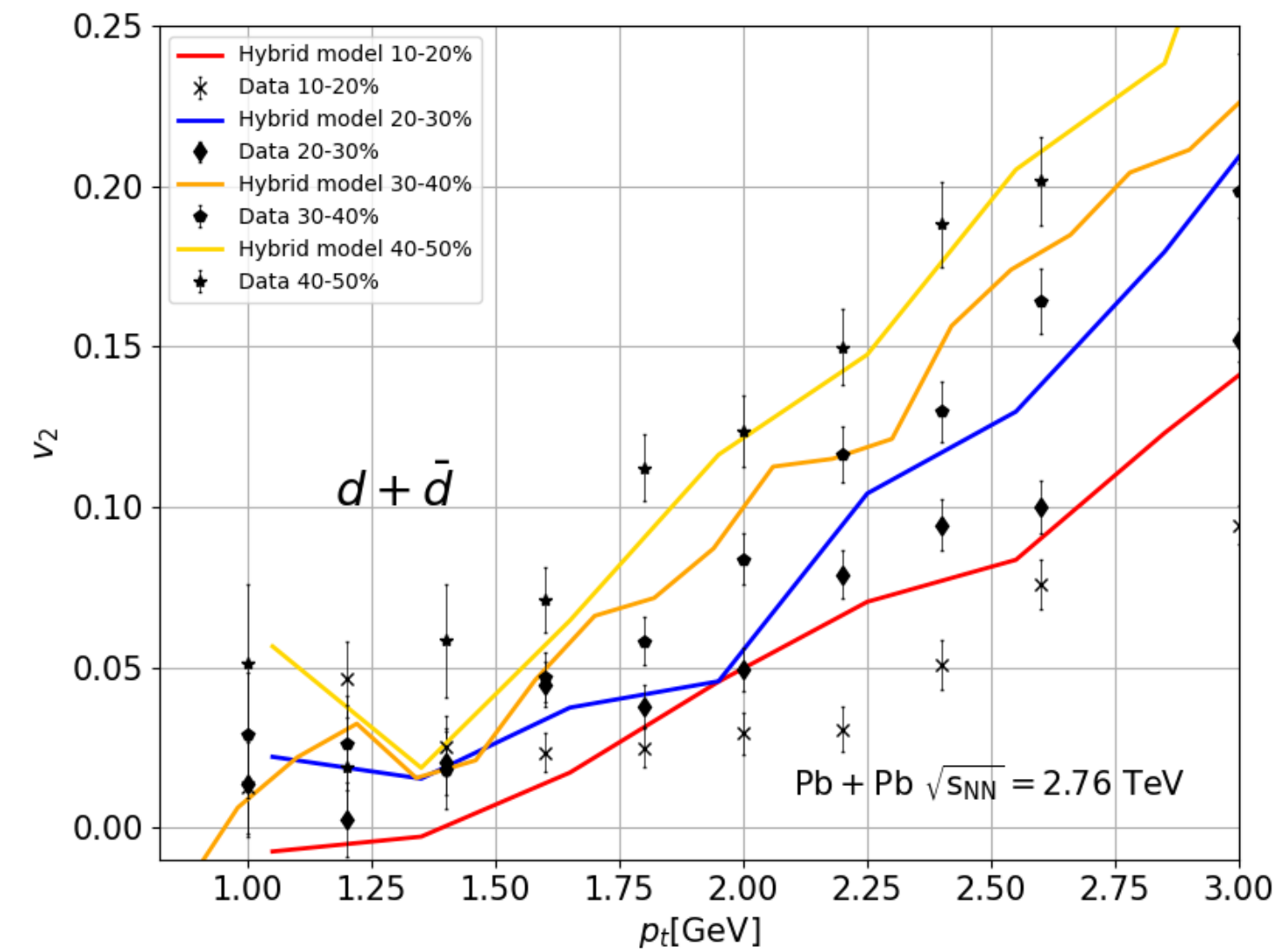
- Spectra in p_t
- $v_2(p_t)$ increases with p_t
- Agreement observed $v_2(p_t)$ for kaons, pions, and protons
- Centrality effects are captured well by the model

- **Prediction of direct deuterons production**

- Intermediate p_t discrepancies noted for deuterons
- First results for coalescence

- **Conclusion and outlook:**

- The hybrid model demonstrates overall good agreement $v_2(p_t)$ with data, especially for kaons, protons, and pions
- Outlook:
 - We aim to incorporate explicit coalescence models into the hybrid framework to compare predictions for deuterons



Thermodynamic relations for perfect spin hydrodynamics

Mykhailo Hontarenko

Institute of Theoretical Physics, Jagiellonian University, PL-30-348 Kraków,
Poland

02-06.12.2024, 24th Zimányi School, Budapest

based on: **W. Florkowski + MH**, arXiv:2405.03263 and
Z. Drogosz + WF + MH, Phys.Rev.D 110 (2024) 9, 096018



NATIONAL SCIENCE CENTRE
POLAND

The problem to be solved

The usual Israel-Stewart approach with spin uses a phenomenological form of scalar thermodynamic relations multiplied by u^μ , where $\omega_{\alpha\beta} = \Omega_{\alpha\beta}/T$ is the spin polarization tensor, thus, from

$$\varepsilon + P = T\sigma + \mu n + \frac{1}{2}\Omega_{\alpha\beta}S^{\alpha\beta} \quad (1)$$

we obtain

$$S_{\text{eq}}^\mu = P\beta^\mu - \xi N_{\text{eq}}^\mu + \beta_\lambda T_{\text{eq}}^{\lambda\mu} - \frac{1}{2}\omega_{\alpha\beta}S_{\text{eq}}^{\mu,\alpha\beta}, \quad (2)$$

$$dS_{\text{eq}}^\mu = -\xi dN_{\text{eq}}^\mu + \beta_\lambda dT_{\text{eq}}^{\lambda\mu} - \frac{1}{2}\omega_{\alpha\beta}dS_{\text{eq}}^{\mu,\alpha\beta}, \quad (3)$$

$$d(P\beta^\mu) = N_{\text{eq}}^\mu d\xi - T_{\text{eq}}^{\lambda\mu} d\beta_\lambda + \frac{1}{2}S_{\text{eq}}^{\mu,\alpha\beta} d\omega_{\alpha\beta}. \quad (4)$$

where the spin tensor is $S^{\lambda,\mu\nu} = u^\lambda S^{\mu\nu}$. Two problems exist:

1) $S_{\text{eq}}^{\lambda,\mu\nu}$ usually has additional terms. 2) If $\omega_{\mu\nu} \sim S^{\mu\nu} \sim \mathcal{O}(\partial^1)$, the spin tensor in (1) should be neglected.

Our solution

Kinetic theory + proper counting scheme leads to:

$$S_{eq}^\mu = \mathcal{N}^\mu - \xi N_{eq}^\mu + \beta_\lambda T_{eq}^{\lambda\mu} - \frac{1}{2}\omega_{\alpha\beta} S_{eq}^{\mu,\alpha\beta}, \quad \mathcal{N}^\mu = \text{coth}(\xi) N_{eq}^\mu \neq P\beta^\mu,$$

$$dS_{eq}^\mu = -\xi dN_{eq}^\mu + \beta_\lambda dT_{eq}^{\lambda\mu} - \frac{1}{2}\omega_{\alpha\beta} dS_{eq}^{\mu,\alpha\beta}, \quad (5)$$

$$d\mathcal{N}^\mu = N_{eq}^\mu d\xi - T_{eq}^{\lambda\mu} d\beta_\lambda + \frac{1}{2}S_{eq}^{\mu,\alpha\beta} d\omega_{\alpha\beta}, \quad (6)$$

$$N_{eq}^\mu = \bar{n}u^\mu + n_t t^\mu, \quad (7)$$

$$T_{eq}^{\mu\nu} = \bar{\varepsilon}u^\mu u^\nu - \bar{P}\Delta^{\mu\nu} + P_k k^\mu k^\nu + P_\omega \omega^\mu \omega^\nu + P_t (t^\mu u^\nu + t^\nu u^\mu). \quad (8)$$

And spin current tensor includes an ortogonal parts to u^λ .

$$S_{eq}^{\lambda,\mu\nu} = u^\lambda S^{\mu\nu} + \text{smth}^{\lambda,\mu\nu}. \quad (9)$$

Boost-invariant spin hydrodynamics with spin feedback effects

Zbigniew Drogosz, Wojciech Florkowski, Natalia Łygan, Radosław Ryblewski
arXiv:2411.06154

Natalia Łygan

Institute of Theoretical Physics, Jagiellonian University,
Kraków, Poland

December 5, 2024



Our approach to spin hydrodynamics

- **motivation: spin polarization measurements in RHIC**

- 1 perfect spin hydrodynamics conserves the spin part of the total angular momentum,
- 2 spin-orbit interaction is dissipative (not included here),
- 3 two-fold expansion: in the magnitude of $\omega_{\mu\nu}$ and gradients,
- 4 my talk: perfect spin hydrodynamics for Bjorken expansion with second-order corrections ¹,

- **boost-invariant and transversely homogeneous system with polarization tensor decomposed to**

$$\omega_{\mu\nu} = k_\mu U_\nu - k_\nu U_\mu + t_{\mu\nu}, \quad t_{\mu\nu} = \epsilon_{\mu\nu\alpha\beta} U^\alpha \omega^\beta, \quad (1)$$

$$k^\mu = C_{kx} X^\mu + C_{ky} Y^\mu + C_{kz} Z^\mu, \quad \omega^\mu = C_{\omega z} X^\mu + C_{\omega y} Y^\mu + C_{\omega z} Z^\mu, \quad t^\mu = V_x X^\mu + V_y Y^\mu + V_z Z^\mu, \quad (2)$$

- calculations with respect to **conservation laws**

$$\partial_\mu N^\mu(x) = 0, \quad \partial_\mu T^{\mu\nu} = 0, \quad \partial_\lambda S^{\lambda,\mu\nu} = 0, \quad (3)$$

- **result: overdetermined system** \Rightarrow additional symmetry \Rightarrow mathematically allowed solutions

- 1 **longitudinal configuration**

$$\mathbf{C}_k = (0, 0, C_{kz}), \quad \mathbf{C}_\omega = (0, 0, C_{\omega z}), \quad (4)$$

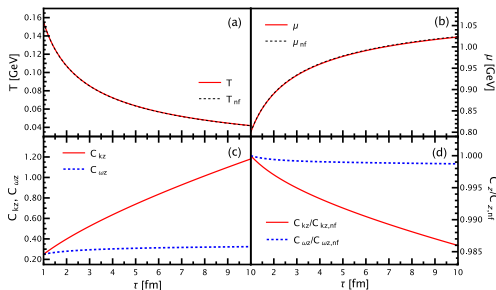
- 2 **transverse configuration**

$$\mathbf{C}_k = (C_{kx}, C_{ky}, 0), \quad \mathbf{C}_\omega = \lambda \mathbf{C}_k. \quad (5)$$

¹Extension of work - W. Florkowski, A. Kumar, R. Ryblewski, R. Singh, *Spin polarization evolution in a boost invariant hydrodynamical background*, Phys. Rev. C 99, 044910 (2019), arXiv:1901.09655.

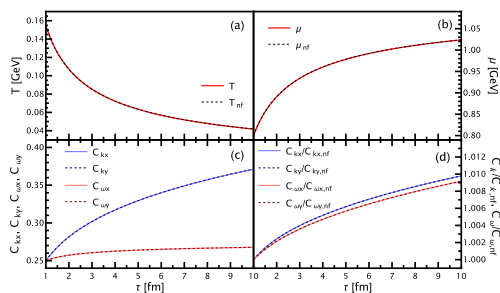
1 Longitudinal configuration

$$C_{kz}^0 = C_{\omega z}^0 = 0.25$$



2 Transverse configuration

$$C_{kx}^0 = C_{ky}^0 = C_{\omega x}^0 = C_{\omega y}^0 = 0.25$$



References

- [1] Zbigniew Drogosz, Wojciech Florkowski, Natalia Łygan, Radosław Ryblewski, *Boost-invariant spin hydrodynamics with spin feedback effects* (2024), arXiv:2411.06154.
- [2] J. D. Bjorken, *Highly relativistic nucleus-nucleus collisions: The central rapidity region*, Physical review D 27, 140 (1983).
- [3] W. Florkowski, A. Kumar, R. Ryblewski, and R. Singh, *Spin polarization evolution in a boost invariant hydrodynamical background*, Phys. Rev. C 99, 044910 (2019), arXiv:1901.09655.
- [4] W. Florkowski, *Phenomenology of Ultra-Relativistic Heavy-Ion Collisions* (2010).
- [5] W. Florkowski and M. Hontarenko, *Generalized thermodynamic relations for perfect spin hydrodynamics* (2024), arXiv:2405.03263.
- [6] Z. Drogosz, W. Florkowski, and M. Hontarenko, *Hybrid approach to perfect and dissipative spin hydrodynamics* (2024), arXiv:2408.03106.

Event-activity-dependent beauty-baryon enhancement in simulations with color junctions

arXiv:2408.16447 [hep-ph]

Lea Virág Földvári, Róbert Vértesi and Zoltán Varga

foldvari.lea.virag@wigner.hu



HUN
REN



December 5., 2024., Budapest, Zimanyi School Winter Workshop

Event-activity-dependent beauty-baryon enhancement in simulations with color junctions

Lea Virág Földvári^{1,2}, Zoltán Varga^{1,3} and Róbert Vértesi¹

foldvari.lea.virag@wigner.hu arXiv:2408.16447 [hep-ph]

1. Heavy-flavor production

- Total cross section of the process calculated by the factorization theorem:

$$\sigma_{\text{had}} = \int f(x_1, Q^2) \otimes f(x_2, Q^2) \otimes \hat{\sigma}_{\text{hard}} \otimes D_{\text{had}}(z, Q^2)$$
- Parton distribution functions (PDFs)
- Partonic hard scattering cross section**
- Fragmentation function**
 - The fragmentation function is traditionally assumed to be universal among different collisional systems
 - It is often computed from e^+e^- collisions
 - However the N_{ch}^B and N_{ch}^D yield ratios:
 - Do not show enhancement in e^+e^- collisions
 - Show a multiplicity dependent enhancement in mid- p_T regime in pp collisions
 - Possible explanation:** Color Reconnection Beyond Leading Color (CR-BLC)

2. PYTHIA models and event multiplicity

- $|\eta| < 1, |y| < 1, p_T > 0.15 \text{ GeV}/c$
- PYTHIA models:
 - CR models allow color string junctions
 - Charm: best described by CR-BLC mode 2
 - Beauty: best described by CR-QCD
- Event multiplicity: N_{ch}
- Number of final state charged hadrons
- N_{ch} dependent enhancement

3. Event classifiers

- Transverse event activity: R_T**
 - Represents the underlying event (UE)
 - Near-side jet-cone activity: R_{NC}
 - Represents the activity within the jet
 - Trigger hadron ($p_T > 5 \text{ GeV}/c$) is required
$$R_T = \frac{N_{\text{near}}}{N_{\text{near}} + N_{\text{trigger}}}$$

$$R_{\text{NC}} = \frac{N_{\text{near}}}{N_{\text{near}} + N_{\text{trigger}}}$$

- Transverse sphericity: S_T**
 - Measures if the event is jetty or isotropic
 - Trigger hadron is not required
 - Concentrates on the midrapidity
$$S_T = \frac{\sigma^2}{\sum_i p_{T,i}^2}$$

- Flattenticity: p**
 - Measures if the event is "hedgohg-like" or jetty
 - Trigger hadron is not required
 - Measures the full rapidity range ($|\eta| < 4$)

4. Results

Transverse event activity and Near-side jet-cone activity

The enhancement is stronger when the R_T is higher, but it does not depend on the R_{NC} .

Transverse sphericity

The enhancement is stronger when the transverse sphericity is higher.

Flattenticity

The enhancement is stronger when the flattenticity is lower.

Summary

- The universality of the fragmentation function is violated
- The beauty is best described by CR-QCD, the charm is best described by CR-BLC mode 2
- CR models: heavy flavor (HF) baryon enhancement comes from the **underlying event**, not the jet
- Flattenticity is strongly related to multiparton interactions and free from biases caused by mid-rapidity jet production
- Using these methods on Run-3 data can reveal further information on the source of the HF-baryon enhancement and help test the validity of different models

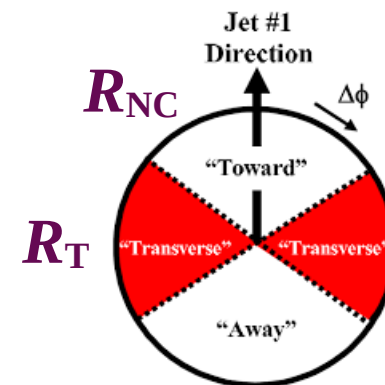
This work has been supported by the Hungarian NKFIH OTKA FK131979 and K135515, 2021-4.1.2-NEMZ_KI-2022-00034.

Event activity classifiers

- **Transverse event activity: R_T**
 - Represents the **underlying event** (UE)
- **Near-side jet-cone activity: R_{NC}**
 - Represents the activity within the **jet**
 - Trigger hadron ($p_T > 5 \text{ GeV}/c$) is required

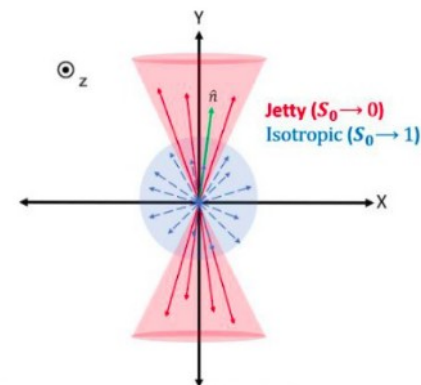
$$R_T = \frac{N_{\text{trans}}}{\langle N_{\text{trans}} \rangle}$$

$$R_{NC} = \frac{N_{\text{cone}}}{\langle N_{\text{cone}} \rangle}$$



- **Transverse spherocity: S_0**
 - Measures if the event is jetty or isotropic
 - Trigger hadron is **not** required
 - Concentrates on the **midrapidity**

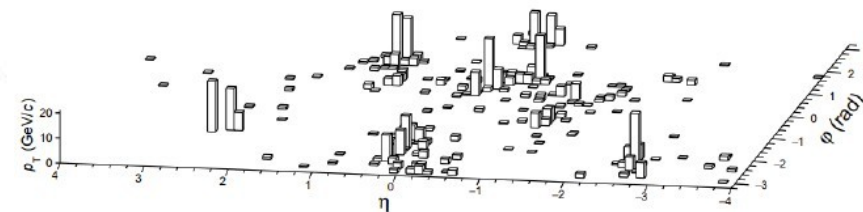
$$S_0 = \frac{\pi^2}{4} \left(\frac{\sum_i |p_{T_i} \times \vec{n}|}{\sum_i p_{T_i}} \right)^2$$



- **Flattenicity: ρ**
 - Measures if the event is “hedgehog-like” or jetty
 - Trigger hadron is **not** required
 - Measures the **full rapidity** range $|\eta| < 4$

$$\rho = \frac{\sigma_{p_T^{\text{cella}}}}{\langle p_T^{\text{cella}} \rangle}$$

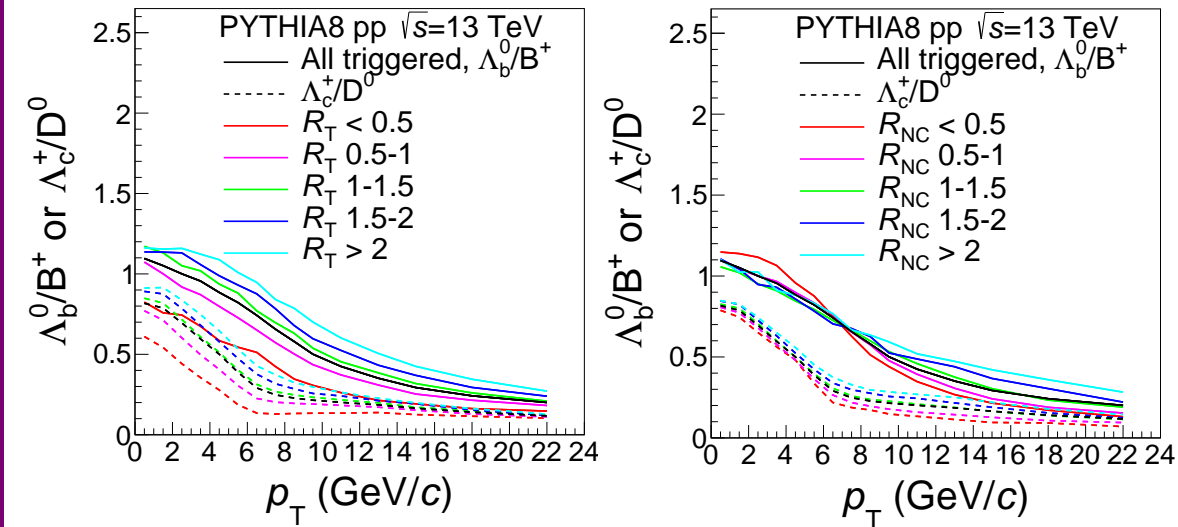
PYTHIA 8.303 (Monash 2013), pp $\sqrt{s} = 13 \text{ TeV}$, $N_{\text{mpi}}=1$, $N_{\text{ch}}=235$, $\rho=1.56$



Results

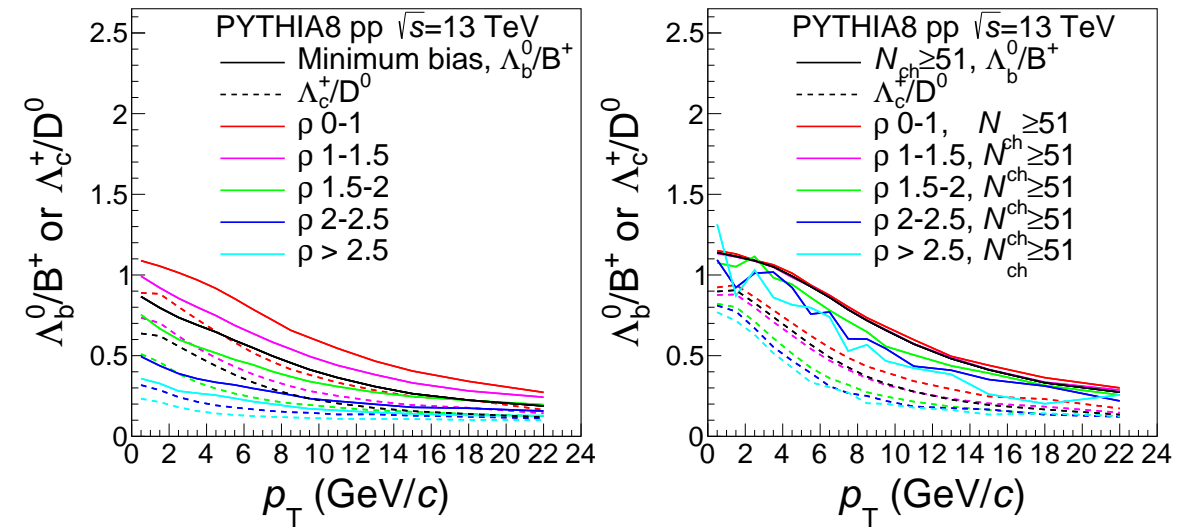
R_T and R_{NC} :

- Activity of the jet \uparrow
- Enhancement does not change
- Activity of the UE \uparrow
- Enhancement \uparrow



Flattenicity:

- Isotropy \uparrow
- Enhancement \uparrow
- **Heavy flavor baryon enhancement comes from the UE**



Review on recent results of J/ψ production at STAR

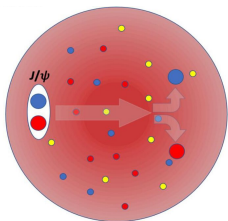
Jitka Mrázková (*for the STAR Collaboration*)

FNSPE, Czech Technical University in Prague

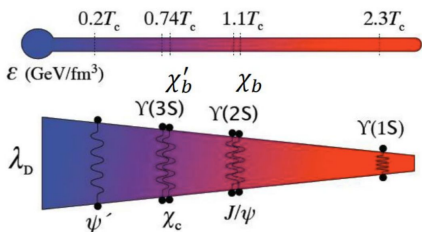
24th ZIMÁNYI SCHOOL
WINTER WORKSHOP
ON HEAVY ION PHYSICS
(December 2-6, 2024)



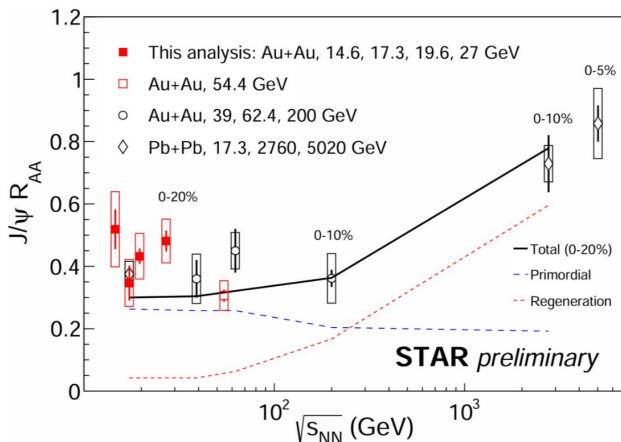
Recent results of J/ψ production in A+A



Credit: Q. Yang (STAR)

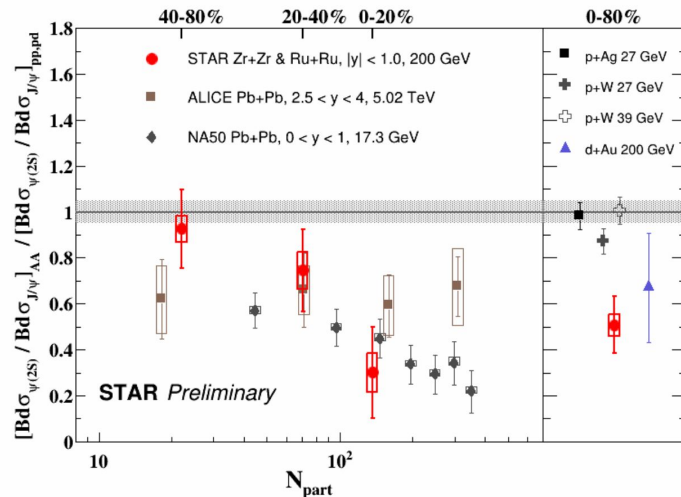


Inclusive J/ψ R_{AA}



No significant energy dependence
in central collisions within
 $\sqrt{s_{NN}} = 14.6 - 200$ GeV

$\psi(2S)$ over J/ψ Double Ratio



First observation of charmonium
sequential suppression in
heavy-ion collisions at STAR

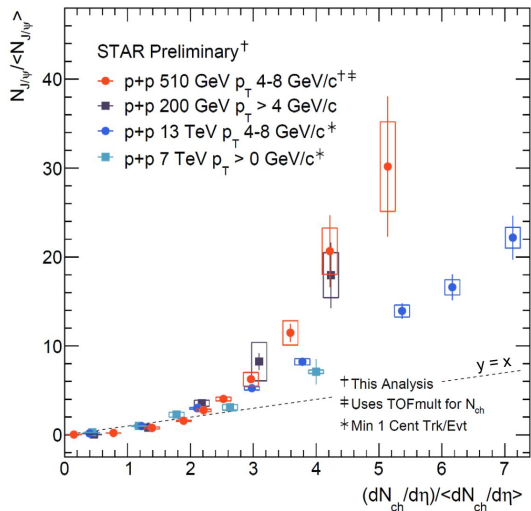
Outlook:

The high luminosity $p+p$ and Au+Au data at 200 GeV from 2023–2025 will enable more precise measurements of $\psi(2S)$ production



Recent results of J/ψ production in $p+p$

J/ψ Production vs Multiplicity in $p+p$

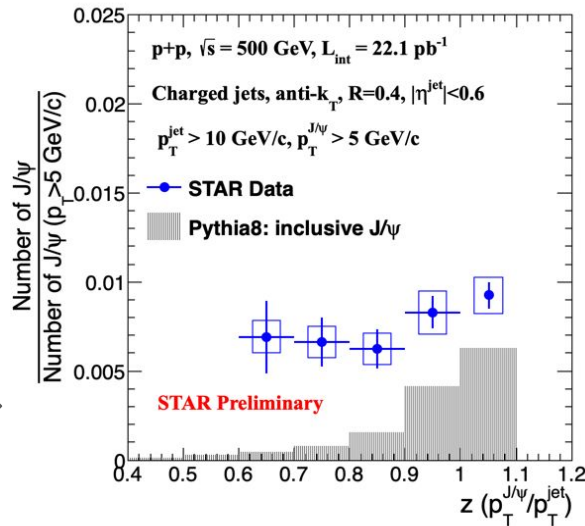


Sign of splitting between results at RHIC and LHC energies

The results show discrepancy with model predictions



J/ψ Production in Jets in $p+p$



Outlook:

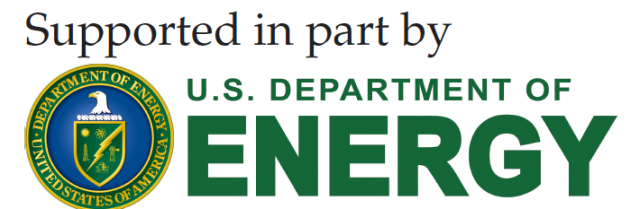
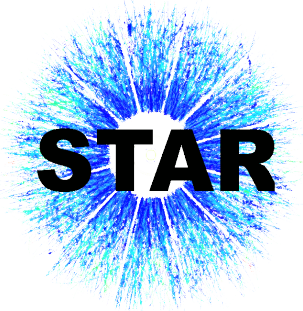
Studies of J/ψ polarization in jets in $p+p$ collisions are ongoing and shall provide deeper insights into the J/ψ production mechanism

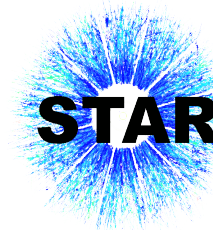


Measurements of D^0 and D^* production in p+p collisions at $\sqrt{s} = 510$ GeV in STAR experiment

Subhadip Pal
(for the STAR Collaboration)

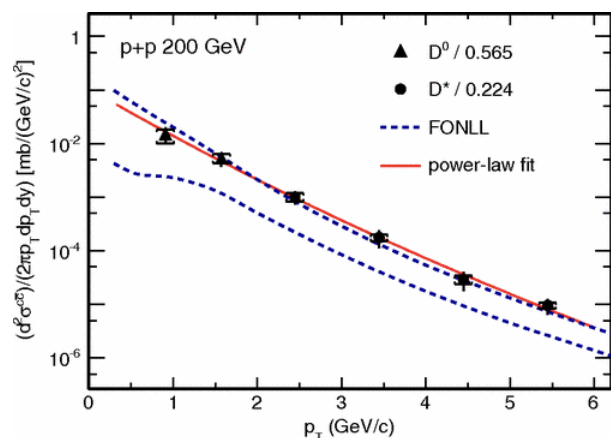
*Faculty of Nuclear Sciences and Physical Engineering
Czech Technical University in Prague*





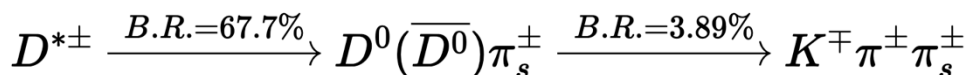
Motivation:

- Studying charm meson production allows for comparisons between experimental results and theoretical models (e.g., perturbative QCD, factorization frameworks).



p_T-differential c c̄ production cross-sections compared with FONLL pQCD calculations

[Phys. Rev. D 86, 072013]

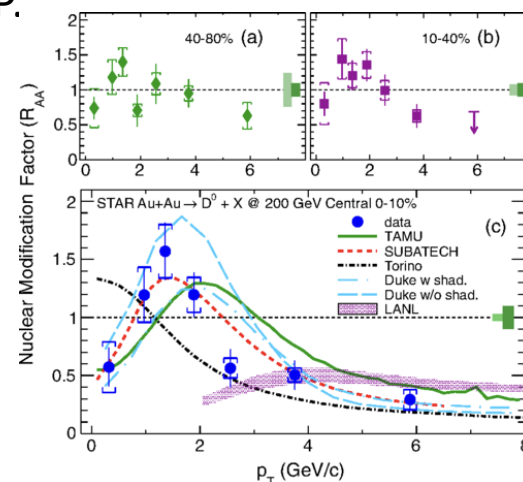


STAR detector:

Time Projection Chamber (TPC): main tracking detector, momentum determination, particle identification via ionization energy loss (dE/dx).

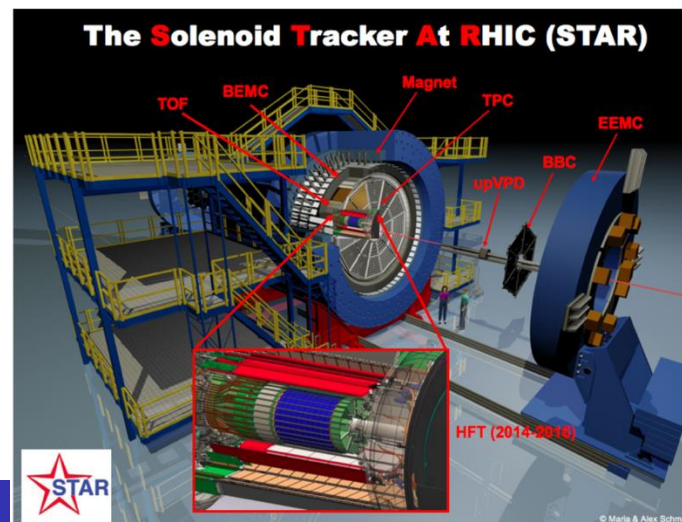
Time Of Flight (TOF): particle identification via velocity (β).

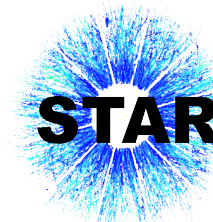
- Modifications of the charm meson production in heavy-ion collisions with respect to p+p provide insights into QGP.



D⁰ meson nuclear modification factor R_{AA}

[Phys. Rev. Lett. 113, 142301]





$$D^{*\pm} \xrightarrow{B.R.=67.7\%} D^0(\overline{D^0})\pi_s^\pm \xrightarrow{B.R.=3.89\%} K^\mp \pi^\pm \pi_s^\pm$$

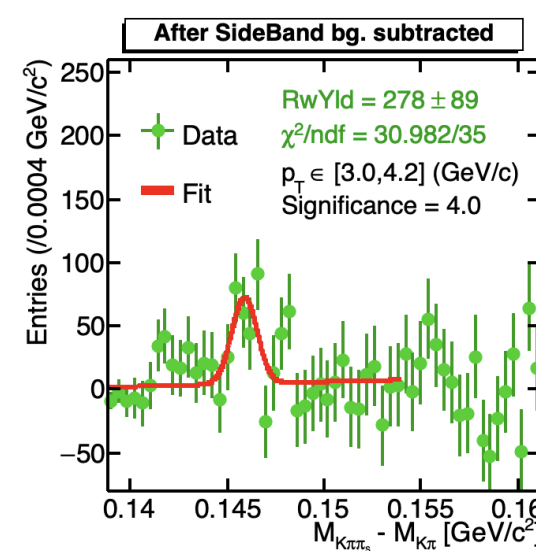
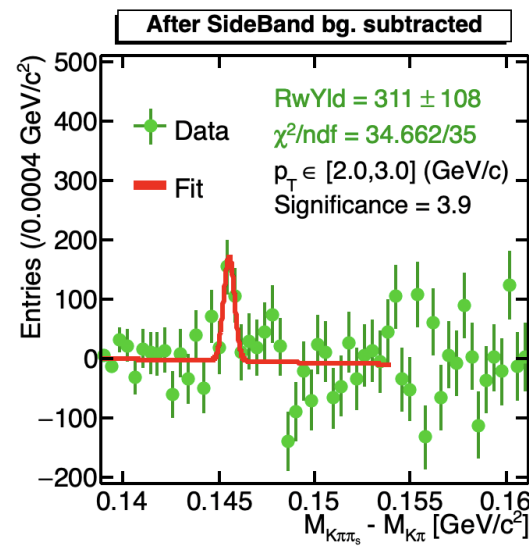
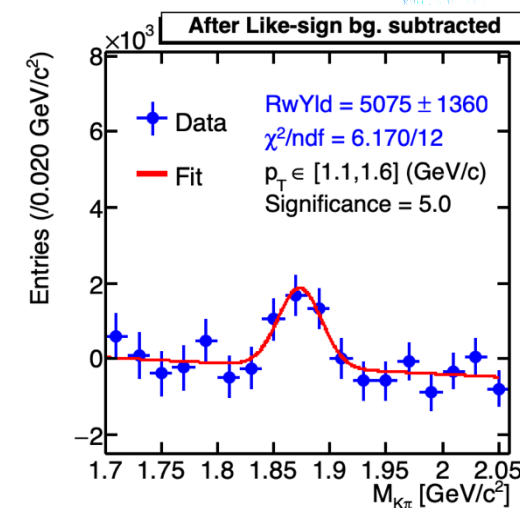
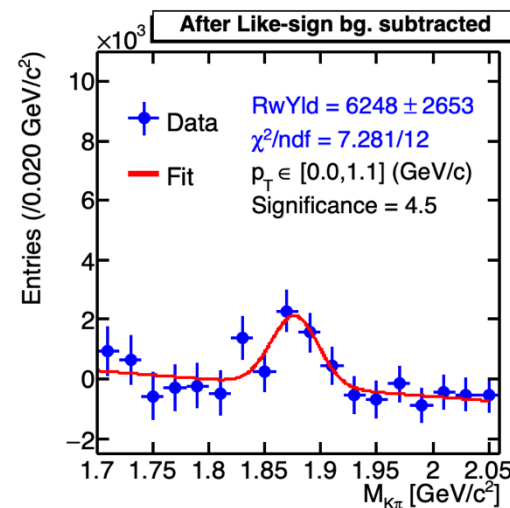
D⁰ signal extraction:

- Unlike-sign pions and kaons are paired.

	$p_T \leq 1.6 \text{ GeV}/c$	$p_T > 1.6 \text{ GeV}/c$
Kaons	$-2.5 < n\sigma_K^{dE/dx} < 3.0$ p dependent cut on $n\sigma_K^{1/\beta}$	$-2.5 < n\sigma_K^{dE/dx} < 3.0$ p dependent cut on $n\sigma_K^{1/\beta}$
Pions	$-3.0 < n\sigma_\pi^{dE/dx} < 3.0$ p dependent cut on $n\sigma_\pi^{1/\beta}$	$-3.0 < n\sigma_\pi^{dE/dx} < 3.0$ if TOF matched p dependent cut on $n\sigma_\pi^{1/\beta}$ if TOF matched $-2.5 < n\sigma_\pi^{dE/dx} < 2.5$ if no TOF info

D^{*} signal extraction:

- Histogram was populated with the mass difference:
 $M_{K\pi\pi_s} - M_{K\pi}$
- Wrong-Sign Combination and Side-Band Method were used to reconstruct background to extract the D^{*} signal.





See you at my poster

Measurements of D^0 and D^* production in p+p collisions at $\sqrt{s} = 510$ GeV in STAR experiment

Subhadip Pal, for the STAR collaboration
Czech Technical University in Prague

CZECH TECHNICAL UNIVERSITY IN PRAGUE

Introduction

This poster is centered around an investigation into the production of D^0 and D^* mesons as a function of transverse momentum (p_T) in proton-proton (p+p) collisions at a center-of-mass energy of $\sqrt{s} = 510$ GeV conducted within the STAR experiment at the Relativistic Heavy Ion Collider (RHIC). The results of this analysis will serve to constrain the charm-anticharm production mechanisms in p+p collisions. We present the ongoing signal extractions of the D^0 and D^* mesons from the minimum bias events recorded during the p+p collisions at $\sqrt{s} = 510$ GeV at STAR in 2017.

Motivation

- Studying charm meson production allows for comparisons between experimental results and theoretical models (e.g., perturbative QCD, factorization frameworks).
- Modifications of the charm meson production in heavy-ion collisions with respect to p+p provide insights into QGP.

p_T -differential c production cross sections compared with FONLL pQCD calculations [1]

D^* meson nuclear modification factor R_{AA} [2]

D^0 Signal Extraction

- Unlike-sign pions and kaons were paired [$K^+\pi^-$, $K^-\pi^+$]
- Two independent background estimation methods were deployed for D^0 signal extraction:
 - like-sign pairs [$K^+\pi^+$, $K^-\pi^-$]
 - track-rotation method [pion tracks are paired with kaon tracks with reversed 3-momentum (180° rotation)]
- Intervals of pair p_T used for the analysis: 0-1.1, 1.1-1.6, 1.6-2.1 GeV/c

Background subtracted data were fitted with Gaussian + linear function.

Raw Yield is extracted from the area under the fitted Gaussian.

STAR Detector

- The STAR detector is excellent in tracking and identifying charged particles at mid-rapidity ($|\eta| < 1$), while providing complete azimuthal coverage.
- The majority of the subsystems are situated within a solenoidal magnetic field of 0.5 T.

- Vertex Position Detector (VPD) to trigger minimum bias events and removing pileup vertices.
- Time Projection Chamber (TPC): main tracking detector, momentum determination, particle identification via ionization energy loss (dE/dx).
- Time Of Flight (TOF): particle identification via velocity (β).

D^* Signal Extraction

- Histogram was populated with the mass difference $M_{\pi\pi^+} - M_{\pi^+}$.
- Wrong-sign combination and side-band method were used to reconstruct background to extract the D^* signal.
- Intervals of the triplet p_T used here are: 2-3, 3-4.2, 4.2-6 GeV/c.

Analysis Method

- About 1.11 billion minimum bias p+p events at $\sqrt{s} = 510$ GeV recorded in 2017 are used in this analysis.
- Hadronic decay channels are used to reconstruct D^0 and D^* .

$D^0(\bar{D}^0) \rightarrow B, R \rightarrow 2, 47\%, K^+\pi^-, K^-\pi^+, D^*(\bar{D}^*) \rightarrow \pi^+\pi^-, \pi^-\pi^+, K^+\pi^+\pi^-, K^-\pi^-\pi^+$

Event Selection		Track Quality Cuts	
$ V_{\text{TPC}} - V_{\text{TOF}} < 4.0$ cm	number of TPC fit points > 18	$V_{\text{TPC}} < 60$ cm	number of hits in plane > 0.52
$V_{\text{TPC}} \in (-0.3, 14)$ cm	global DCA < 1.5 cm	$V_{\text{TOF}} \in (-0.26, 0.02)$ cm	$p_T > 0.2$ GeV/c
	$ \eta < 1$		

PID	
Kaon	$p_T \in [1.6, 6]$ GeV/c $-2.5 < \ln(\frac{dE/dx}{\langle dE/dx \rangle}) < 2.0$ if dependent on $\cos^2\theta$
Pion	$p_T \in [1.6, 6]$ GeV/c $-3.0 < \ln(\frac{dE/dx}{\langle dE/dx \rangle}) < 2.0$ if dependent on $\cos^2\theta$, > 3.0 if TOF matched if dependent on $\cos^2\theta$, > 2.5 if TOF matched

D^0 daughter Kaon and Pion PID Cuts

For Soft Pion (π_s) identification, TOF pion cut was loosened for $p < 1.6$ GeV/c to select more low momentum tracks.

References

- L. Adamczyk et al. (STAR Collaboration), 2012, Phys. Rev. D 86, 072013.
- L. Adamczyk et al. (STAR Collaboration), 2014, Phys. Rev. Lett. 113, 142301

Acknowledgement

The work was supported by the Grant Agency of the Czech Technical University in Prague, grant No. SGS22/174/OHK4/3T/14

Summary and Outlook

- D^0 and D^* signals were extracted up to p_T of 2.1 GeV/c and 6.0 GeV/c, respectively using Minimum Bias p+p data at 510 GeV.
- Analyses were performed with two independent background estimation methods.
- Efficiency and systematic uncertainties to be determined next for cross-section calculation.
- Barrel High Tower triggered data is also being analyzed currently for raw yield measurements at higher p_T .

24th ZIMÁNYI SCHOOL WINTER WORKSHOP ON HEAVY ION PHYSICS, December 2-6 2024; Budapest

STUDY OF UPSILON-PION AZIMUTHAL CORRELATION

Kristýna Šedová

Czech Technical University in Prague - Faculty of Nuclear Sciences and Physical Engineering

- The aim is to study production mechanism of Upsilon
- The bound state is formed through color-singlet or color-octet channel

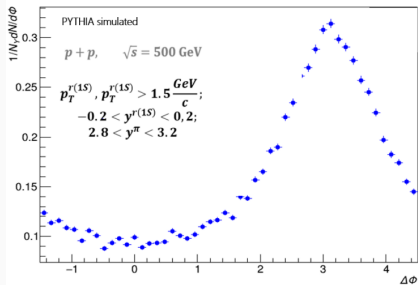


Figure 1: Upsilon-Pion azimuthal correlation using PYTHIA Generator.

Taken from: O. Mezhenka, SQM 2024.

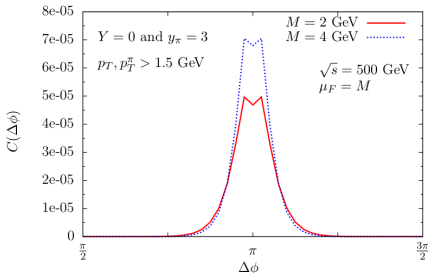


Figure 2: The correlation function $C(\Delta\varphi)$ in p+p collision at $\sqrt{s} = 500$ GeV.

Taken from: E. Basso et al., PoS, EPS-HEP2015, 191 (2016).

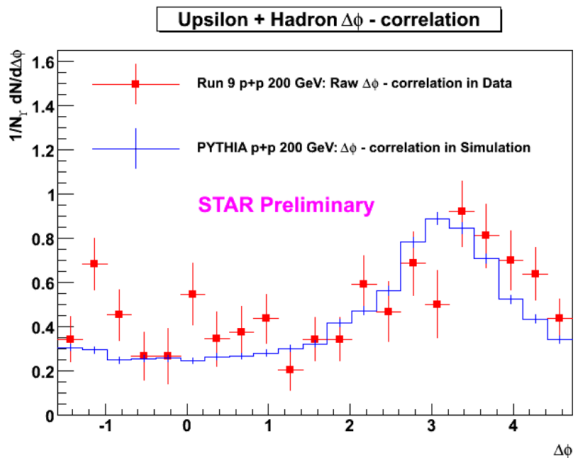


Figure 3: Upsilon-Hadron azimuthal correlation measured by STAR.

Taken from: M. C. Cervantes, J. Phys.: Conf. Ser. 316 012023 (2011).

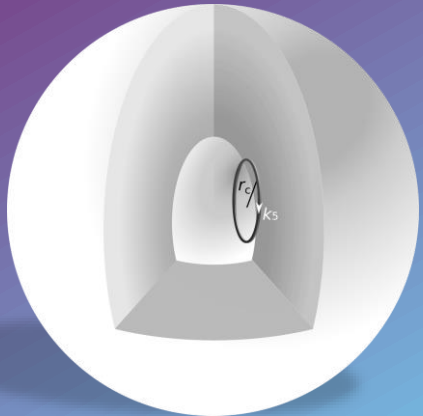


Generalized Uncertainty Principle

$$\Delta x \Delta p \geq \frac{\hbar}{2} + \beta \Delta p^2$$

Extra dimensions and gravity

Thermodynamics and
neutron stars



Black holes and a
Schwarzschild-like solution



EÖTVÖS LORÁND
UNIVERSITY | BUDAPEST

Acknowledgements

This work was supported by Hungarian National Research, Development and Innovation Office (NKFIH) under Contracts No. OTKA K135515, No. NKFIH NEMZ_KI-2022-00031, 2024-1.2.5-TÉT-2024-00022 and Wigner Scientific Computing Laboratory (WSCLAB, the former Wigner GPU Laboratory). Author A.H. is supported by NKFIH through the DKÖP program of the Doctoral School of Physics of Eötvös Loránd University and HUN-REN's Mobility fellowship with identifiers KMP-2023/101 and KMP-2024/31.

Galactic rotation curves with thermodynamic gravity

Máté Pszota

in collaboration with

Péter Ván

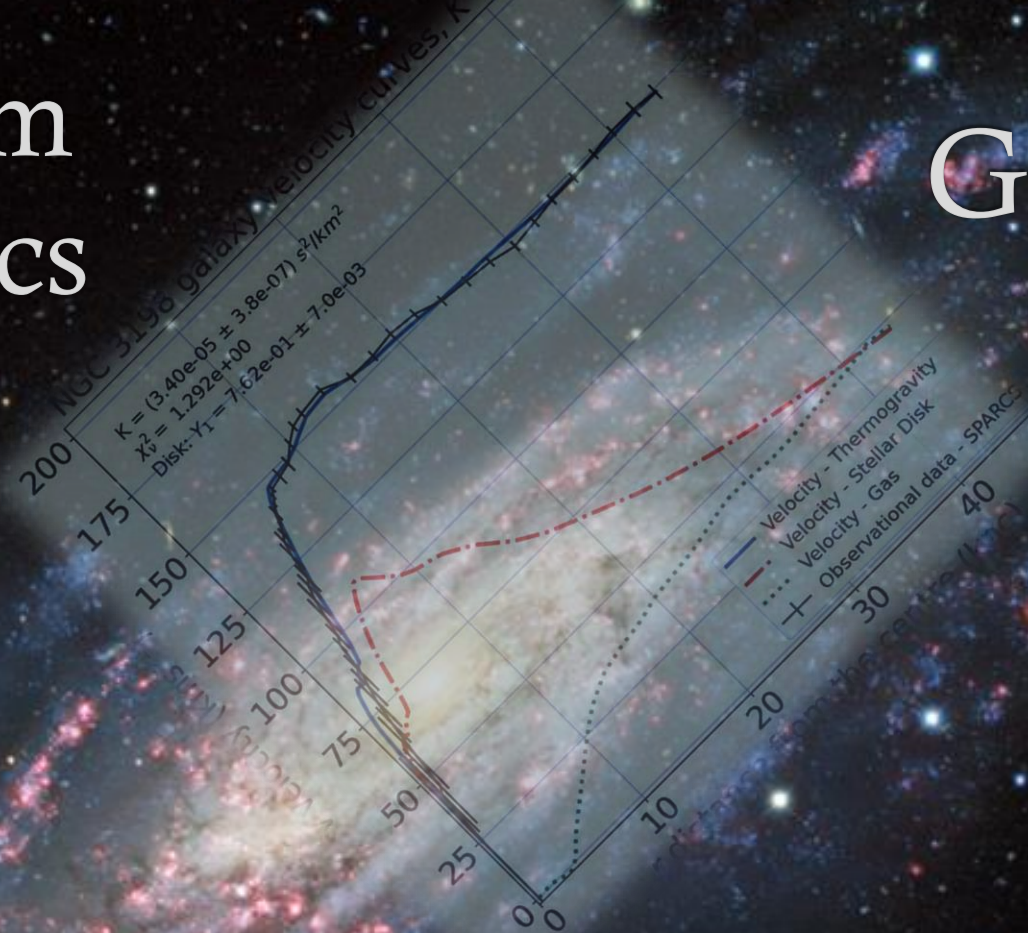
**HUN
REN**



ELTE EÖTVÖS LORÁND
UNIVERSITY

Nonequilibrium thermodynamics

Gravity



$$u = e - \varphi - \frac{\nabla \varphi \cdot \nabla \varphi}{8\pi G \rho}$$

$$\Delta \varphi = 4\pi G \rho + K(\nabla \varphi)^2$$

ZIMÁNYI SCHOOL 2024



24th ZIMÁNYI SCHOOL
WINTER WORKSHOP
ON HEAVY ION PHYSICS
December 2-6, 2024
Budapest, Hungary



József Zimányi (1931 - 2006)

L. Kassák: Image architecture

Drell-Yan measurements at low invariant masses with the upgraded ALICE detector

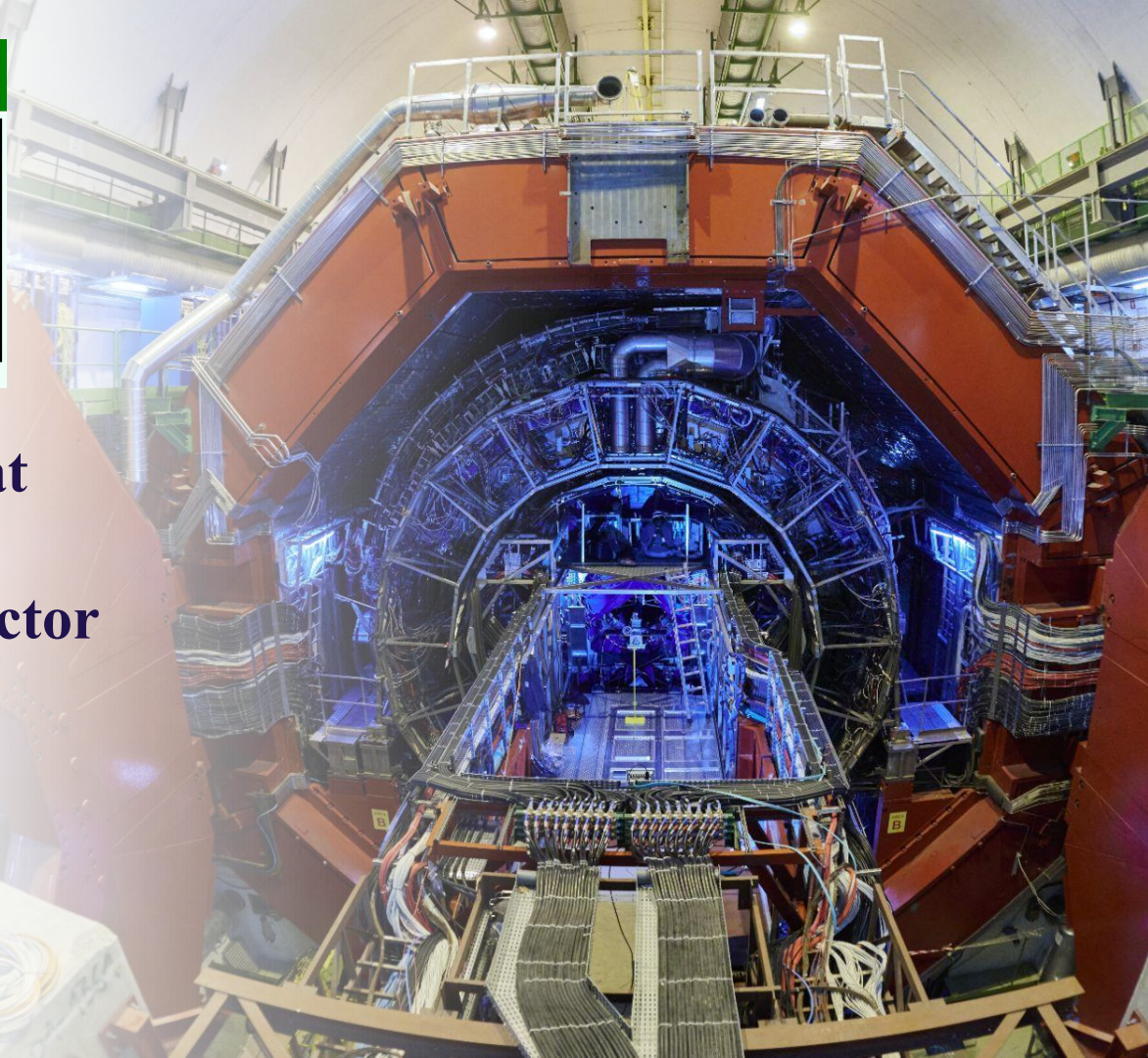
SAHIL UPADHYAYA



THE HENRYK NIEWODNICZAŃSKI
INSTITUTE OF NUCLEAR PHYSICS
POLISH ACADEMY OF SCIENCES
KRAKÓW, POLAND

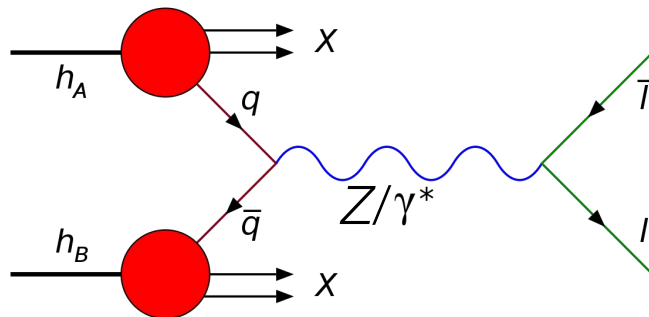


ALICE



Drell-Yan process

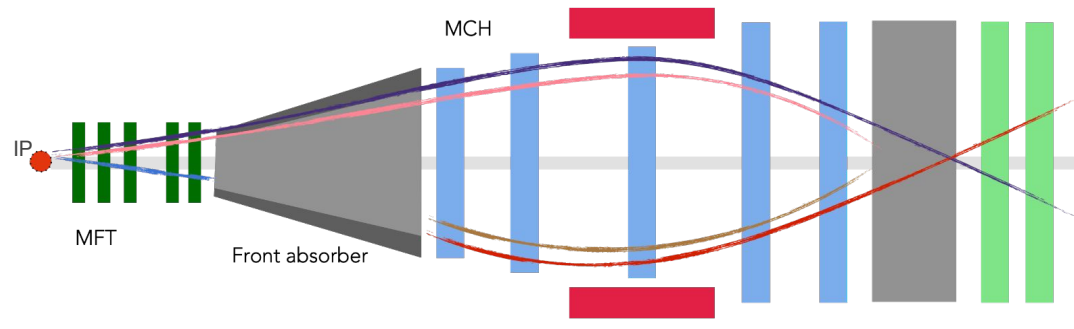
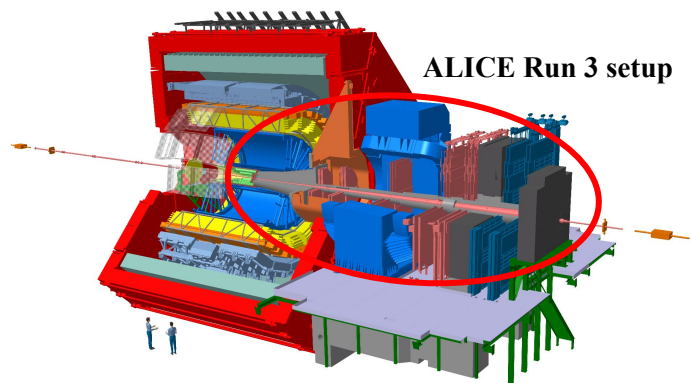
→ The Drell-Yan (DY) process is the production of a **lepton pair** from an **electroweak interaction** of a **quark-antiquark pair** :



→ Measuring the DY process at LHC energies is particularly important to characterize thermodynamic and transport properties of the hot and dense medium created in ultra-relativistic heavy-ion collisions

→ Measurements provide stringent **tests for the theory of perturbative Quantum Chromodynamics (pQCD)** as well as **significant constraints on the evaluation of parton distribution functions (PDFs)**

Drell-Yan measurements with upgraded ALICE



→ Drell-Yan with **ALICE Run 3 setup** → $\mu+\mu-$ detection and tracking in **forward direction** ($-3.6 < \eta < -2.5$) using the **ALICE muon spectrometer**

→ **Goal:** To measure **low-mass DY lepton pairs** (M_{DY} down to $4 \text{ GeV}/c^2$) to constrain nuclear PDFs at small Q^2 and x (**down to 10^{-5}**) where there is lack of data

→ $\sim 10^4$ – **expected Drell-Yan statistics** at forward rapidity in pp with the proposed luminosity (L) $\sim 200/\text{pb}$ (Pythia and NLO calculations for lepton $p_{\text{T}} \sim 3 \text{ GeV}/c$)

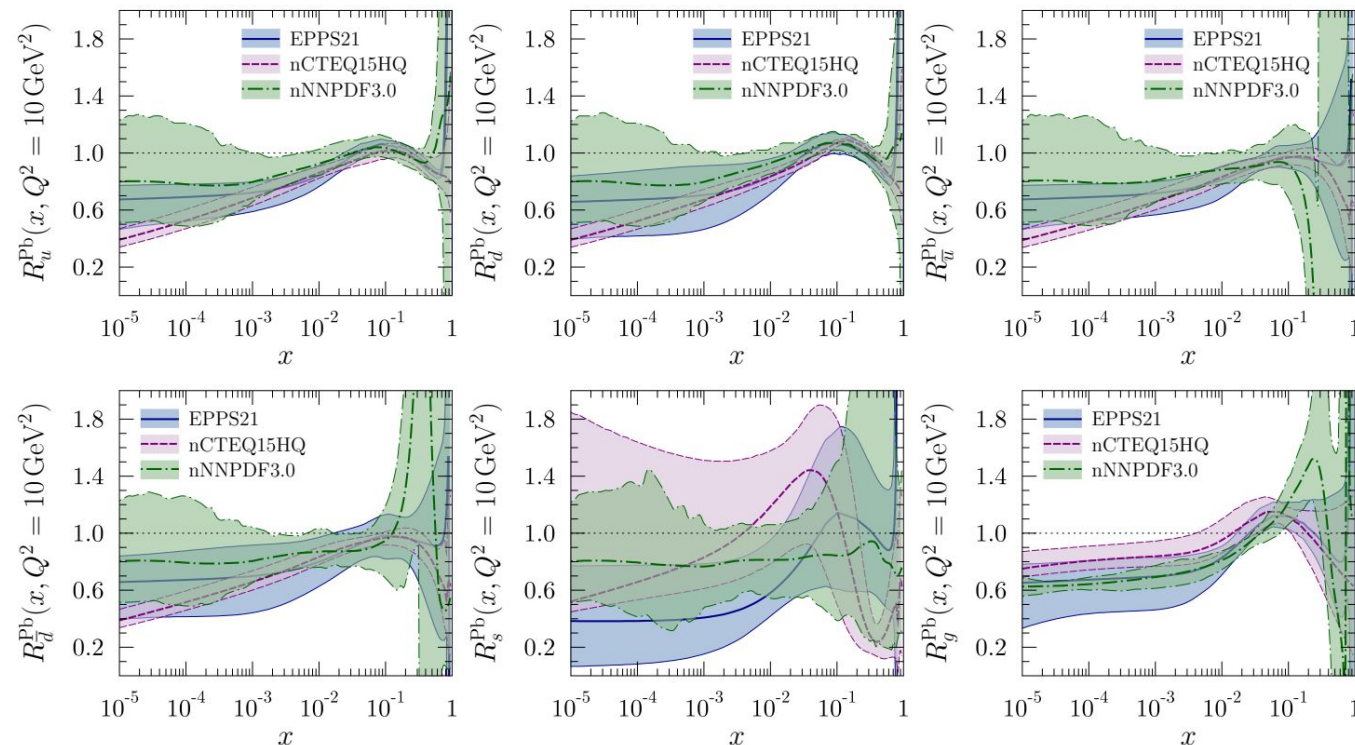
Prospect

→ At small- x , the ratio of the **nuclear modification factors** of DY and J/ψ in **p-Pb collisions** (R_{pPb}) can provide important **constraints on gluon densities**

→ Comparison of the ^{208}Pb nuclear modifications from the EPPS21, nCTEQ15HQ and nNNPDF3.0 global analyses of nuclear PDFs show

large uncertainties for $x < 10^{-3}$

→ **Certainly a need to improve the precision of the low- x calculations**



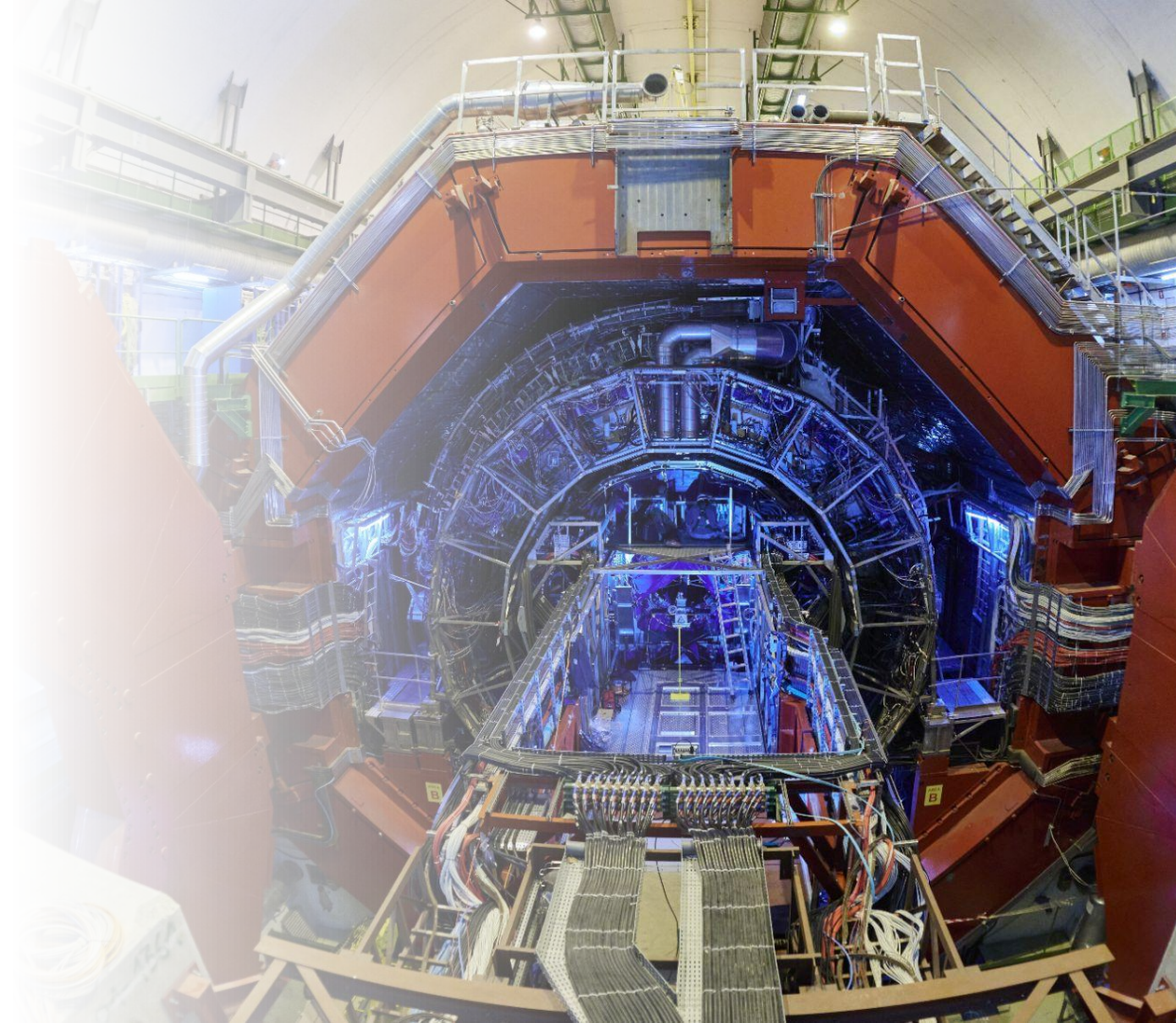


Thank You Köszönöm

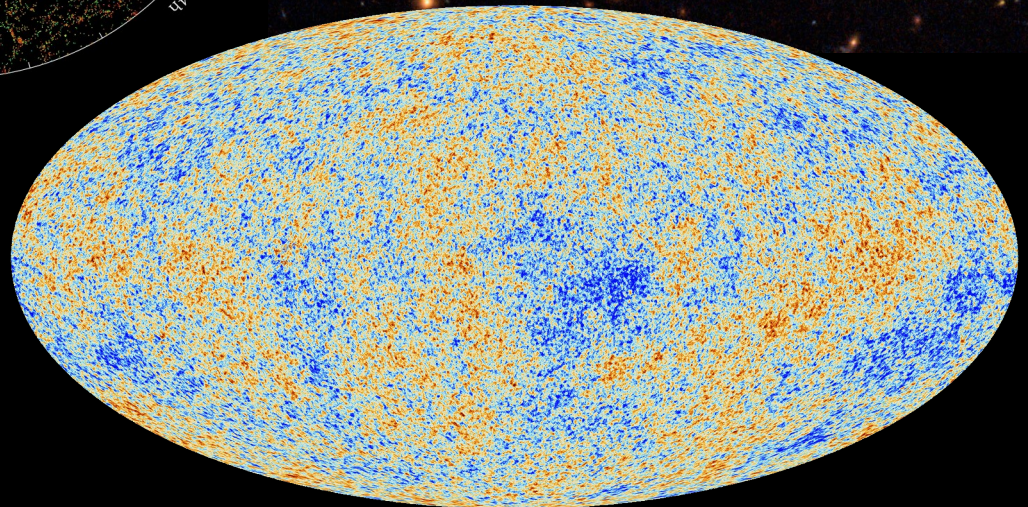
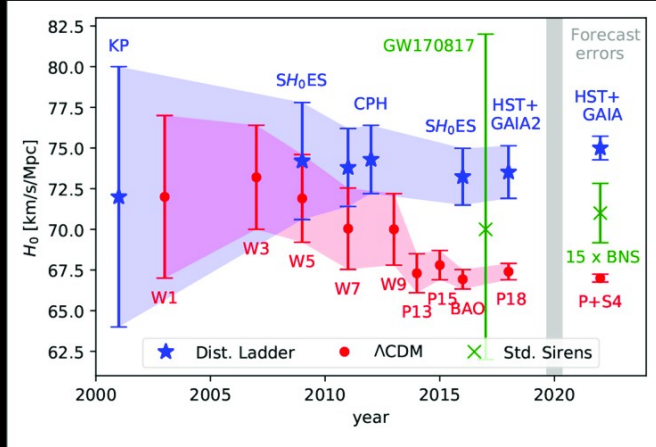
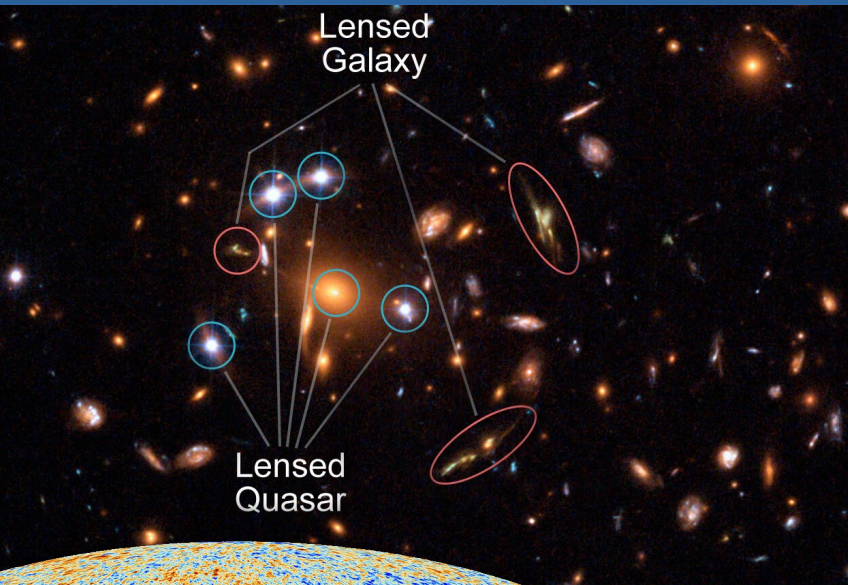
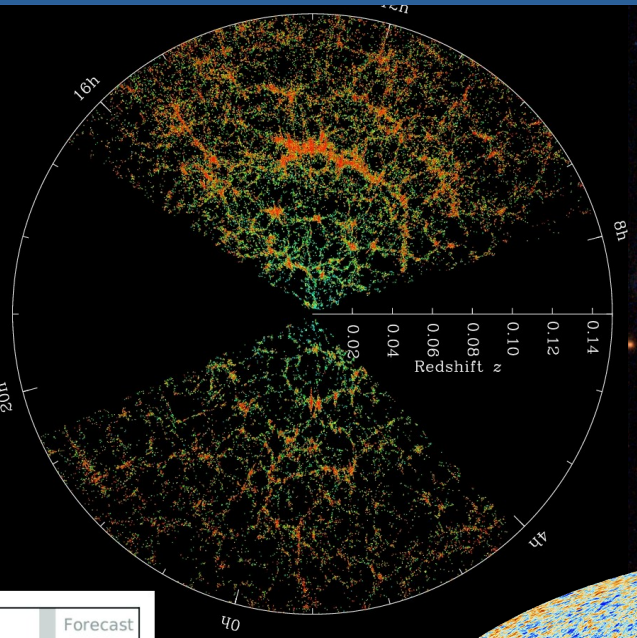
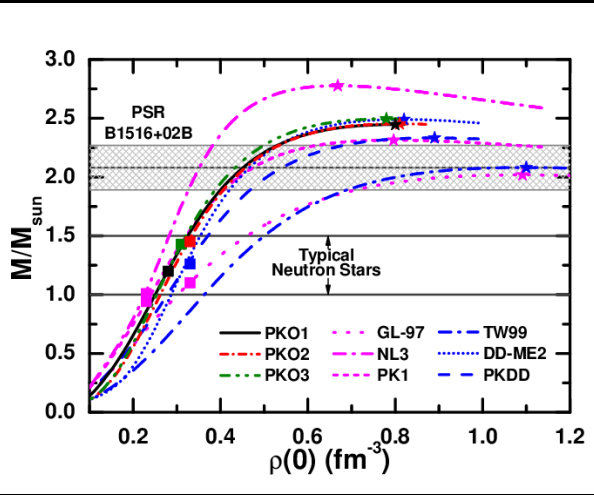
Contribution supported by the Polish Ministry
of Education and Science Grant -
DIR-WSIB.92.11.2023

References:

- [1] Phys. Rev. Lett. **25** 316 (1970)
- [2] ALICE-MFT, CERN-LHCC-2015-001,
ALICE-TDR-018, May 2015
- [3] POWHEG box - powhegbox.mib.infn.it
- [4] CERN-THESIS-2022-319
- [5] Ann. Rev. Nucl. Part. Sci. **60** (2010) 463
- [6] Phys. Rev. D **58** (1998) 074012
- [7] Phys. Rev. D **96** (2017) 094014
- [8] arXiv:2311.00450v2

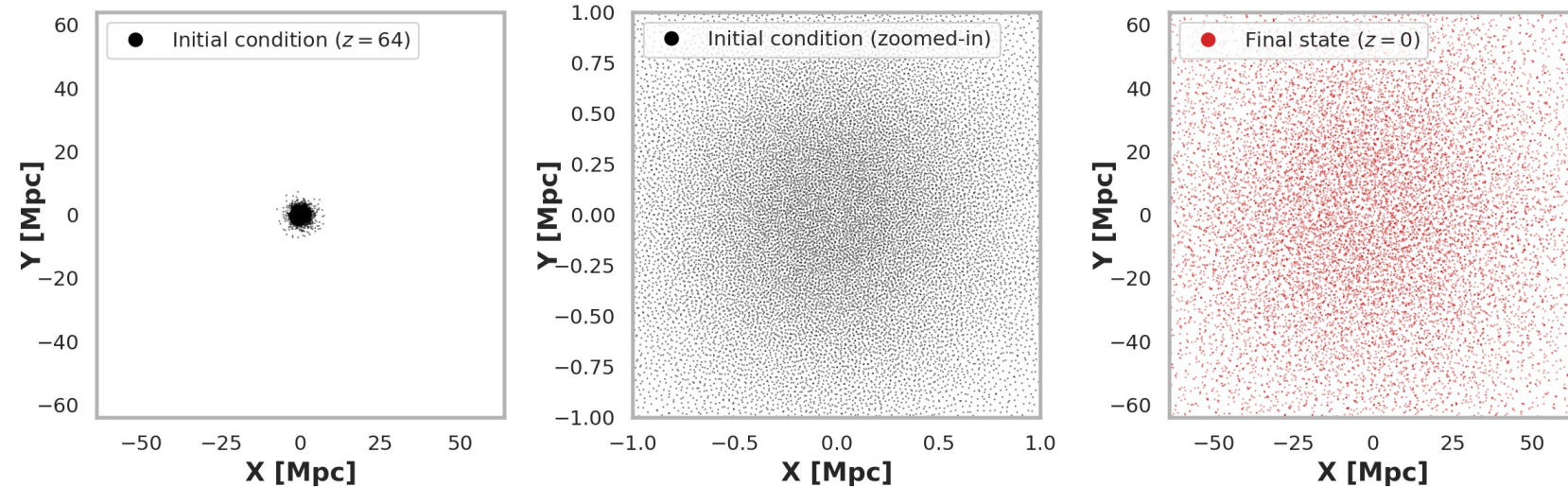


Modern Cosmology

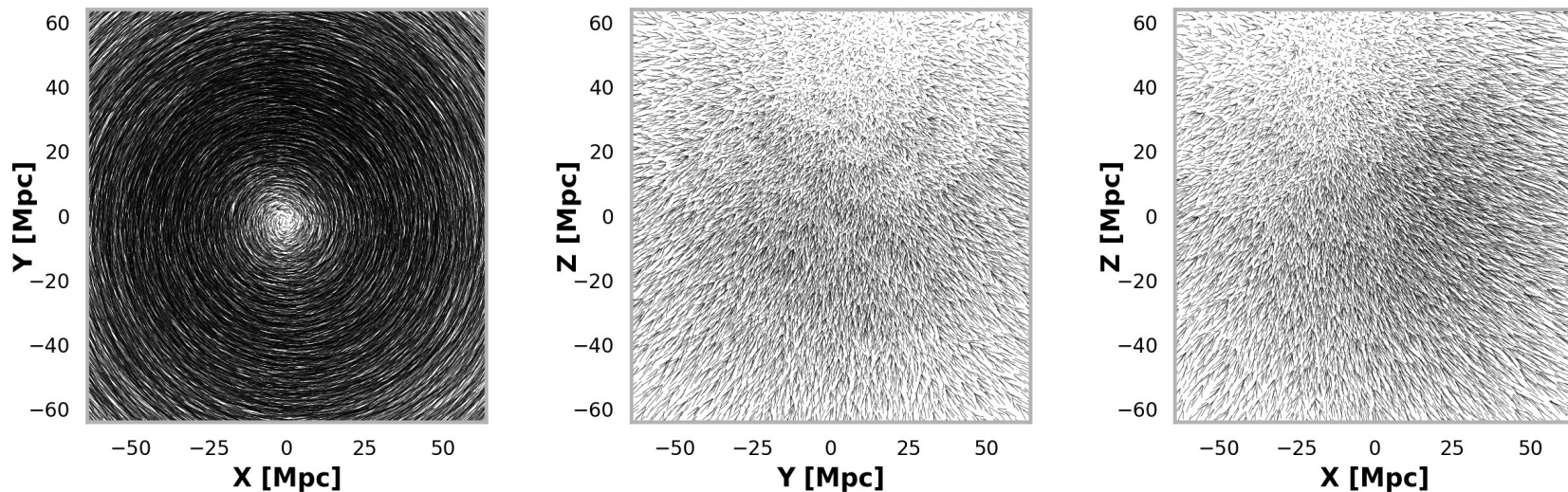


StePS rotating simulation

Evolution



Displacement field



Measuring the expansion of the Universe

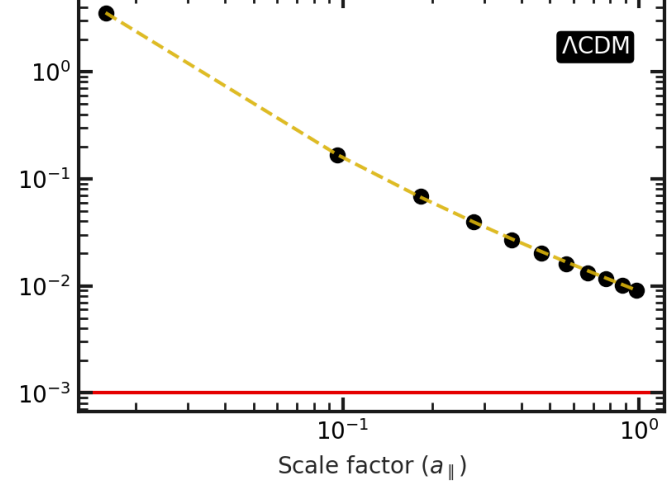
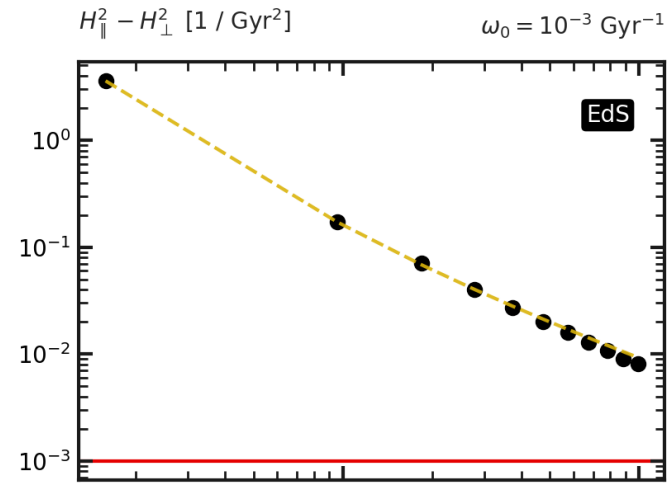
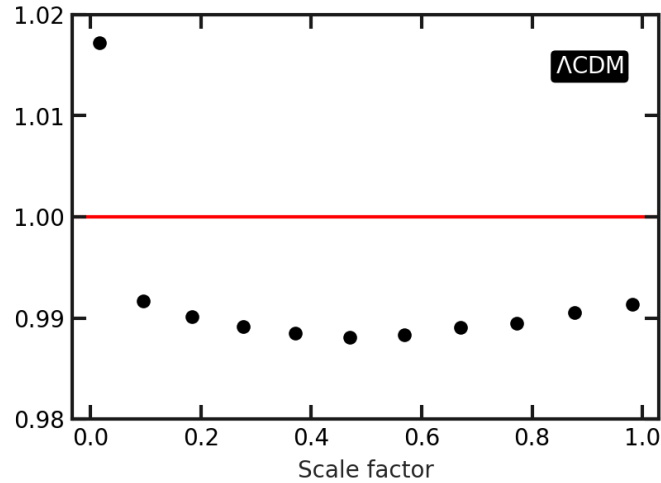
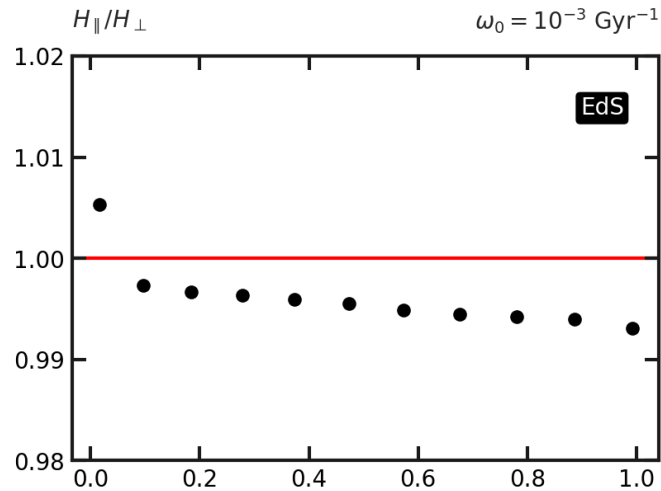
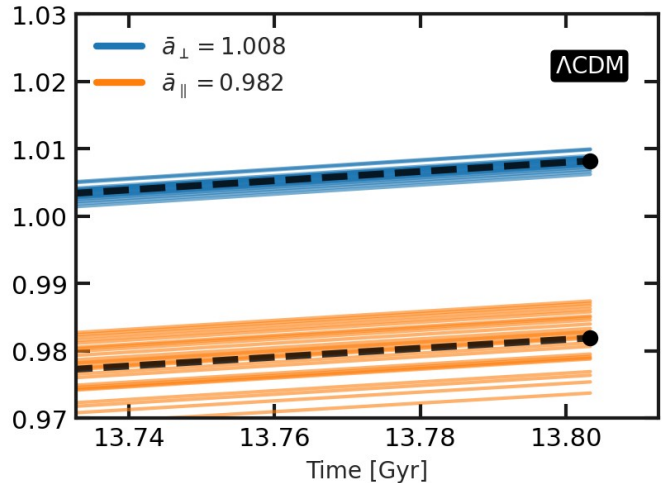
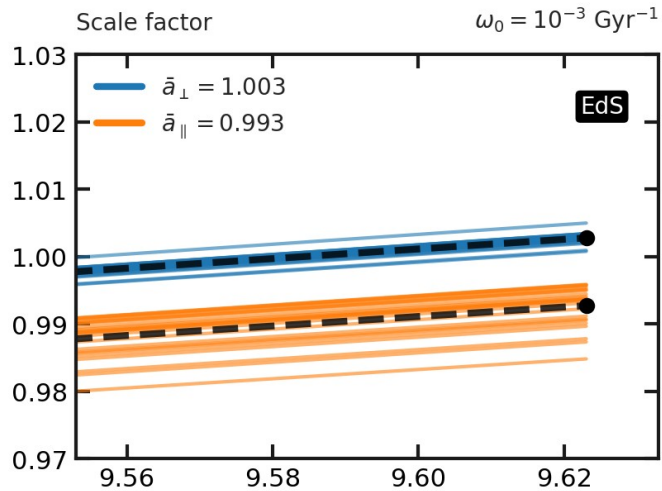


Image reconstruction in proton computed tomography

Zimányi Winter Workshop
on Heavy Ion Physics
Budapest
2-6/12/24

ZSÓFIA JÓLESZ
jolesz.zsofia@wigner.hun-ren.hu

Gábor Bíró
Gábor Papp

ArXiv:2212.00126



EÖTVÖS LORÁND
UNIVERSITY | BUDAPEST



ELTE
EÖTVÖS LORÁND
UNIVERSITY

**IMAGE RECONSTRUCTION WITH PROTON
COMPUTED TOMOGRAPHY**

Zsófia Jólesz¹, Gábor Bíró¹, Gábor Papp¹, Greggy Gábor Burdakov¹

¹HUN-REN Wigner Research Centre for Physics, 29-33 Konkoly-Thege Miklós út, 1121 Budapest
²Eötvös Loránd University, Pázmány Péter Sétány 1/A, H-1117 Budapest.

**24TH ZIMÁNYI
SCHOOL**
BUDAPEST, HUNGARY

DECEMBER 2-6, 2024.

INTRODUCTION

- Proton therapy has outstanding results in cancer therapy due to the protons' nature: they have a very localized dose deposit
- Before every radiotherapy, there is a need for imaging – this is carried out by X-ray CT most of the time – it gives information about the absorption of photons – a conversion is needed to be made from Hounsfield units to proton Relative Stopping Power (RSP) – this results in some errors
- Use the same particle for imaging we use for the treatment – proton CT

THE BERGEN PCT COLLABORATION

The ALPIDE chip

- Aims to build a proton CT based on the high energy particle detectors used in the CERN ALICE Collaboration (technology transfer)
- The detector system is based on the ALPIDE chip (Monolithic Active Pixel Sensor)
- Steps of the imaging: Irradiate patient (~100 MeV protons) – detector senses the signals – process signals – reconstruct the image

The Bergen proton CT

THE RICHARDSON-LUCY ALGORITHM

- Statistical iterative algorithm
- Models the problem as a linear equation system

$$A \cdot X = Y$$

Matrix containing the interaction coefficients between protons and pixels/voxels

Vector containing the known Water Equivalent Path Lengths of the protons

Vector containing the estimated proton RSP values

GOALS AND DEVELOPMENTS

- Hadron therapy is one of the most effective treatments for cancer: less damage in healthy tissues, more dosage in the tumour
- Imaging is a crucial part – but photon CT (used currently in the clinical practice) has its limitations – let's use proton CT – but protons do Coulomb scattering – calculating RSP at voxel level and handling proton trajectories are crucial tasks
- Goals: testing, improving and optimizing a framework which uses the Richardson-Lucy algorithm for imaging
- Generating data with Monte Carlo simulations (Geant4 & GATE) – very time consuming – parallelization
- Comparing 3 different setups: ideal, silicon pixel and silicon strip detector
- Most Likely Path calculation of the protons – using cubic spline approximation
- Grouping data in batches – check MSE between iterations – if < threshold – process data in the next batch

The workflow of the process

SPATIAL RESOLUTION

- Using Derenzo phantom (epoxy cylinder with different sized aluminium rods)
- Evaluating spatial resolution with Modulation Transfer Function: average individual rods – get their point spread function – get MTF with 2D Fourier transformation
- Average MTF_{50%} for the different setups:
 - 1.43 lp/cm (ideal)
 - 1.17 lp/cm (pixel)
 - 0.94 lp/cm (strip)

RSP RECONSTRUCTION

- Using CTP404 phantom (epoxy cylinder with 8 rods of different materials)
- Comparing the reconstructed RSP values of the 3 setups to the ground truth values
- The biggest relative difference between the ground truth and the reconstructed values was ~4%

ACKNOWLEDGEMENTS

My research was supported by the Hungarian National Research, Development and Innovation Office (NKFIH) grants under the contract numbers OTKA K135515 and 2021-4.1.2-NEMZ-KI-2004-00033.

SUMMARY

- We have developed a framework that uses the Richardson-Lucy algorithm for imaging with protons – has never been used for this purpose before
- Reached a significant improvement in the runtime (days – minutes)
- There is still room for improvement in the spatial and the RSP reconstruction, however promising results have been achieved

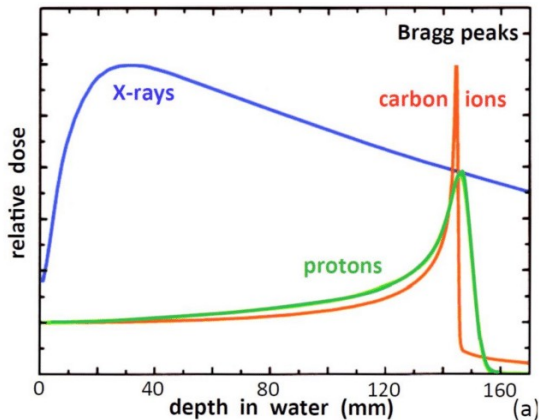
REFERENCES

[1] G. Burdakov, A. Lőrincz, D. János, G. Papp, G. Gábor Burdakov, Proton Computed Tomography Based on the Richardson-Lucy Algorithm, 2024, arXiv:2401.11111v1 [eess.SP]

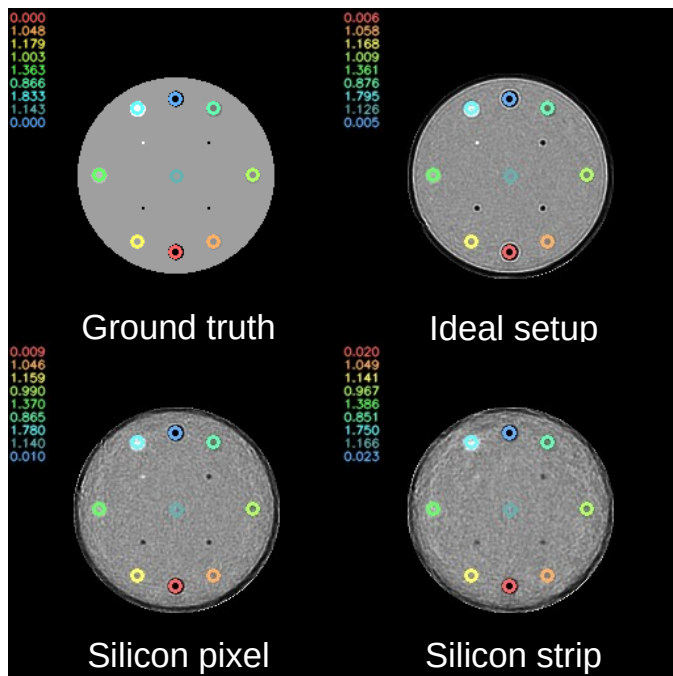
[2] A. Lőrincz et al., A high-precision digital processing pipeline for proton CT, 2024, arXiv:2401.11111v1 [eess.SP]

[3] G. Burdakov, A. Lőrincz, D. János, G. Papp, G. Gábor Burdakov, Proton Computed Tomography Based on the Richardson-Lucy Algorithm, 2024, arXiv:2401.11111v1 [eess.SP]

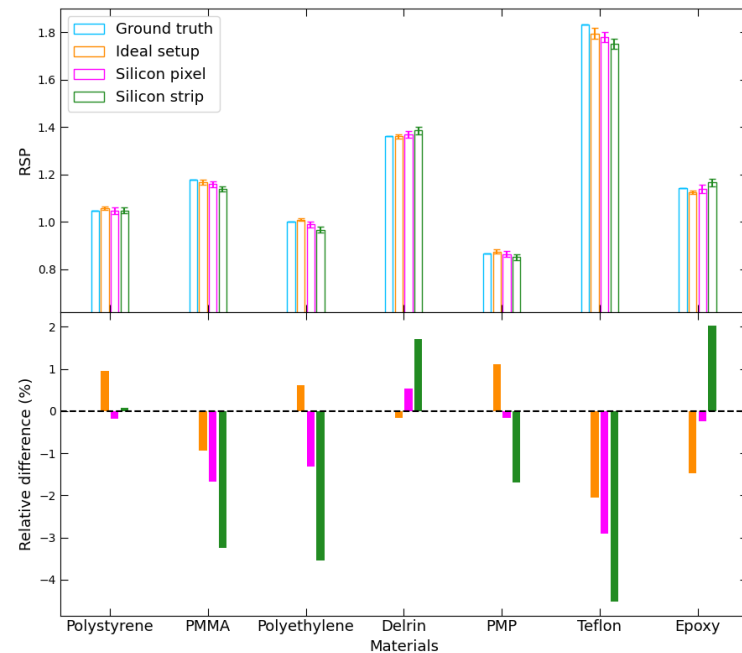
Richardson-Lucy algorithm for imaging



- Protons & heavy ions: Coulomb scattering → Bragg peak → localized dose deposit



- Hadron therapy: outstanding cancer treatment – but there are challenges with the imaging



- First time using Richardson-Lucy algorithm for medical imaging
- Optimizing the framework: speed & accuracy
- Testing the algorithm on 2 phantoms: spatial resolution & RSP reconstruction
- Promising results (using $\sim 10^6$ protons), comparable with other used algorithms

First $d^2\sigma/dp_T dy$ measurement of D^0 photoproduction in PbPb UPCs

**BALÁZS CSABA KOVÁCS (ELTE) ON BEHALF OF THE CMS COLLABORATION
POSTER SESSION, 24. ZIMÁNYI SCHOOL,
2-6 DEC. 2024, BUDAPEST**



EÖTVÖS LORÁND
UNIVERSITY | BUDAPEST





D⁰ photoproduction in UPCs

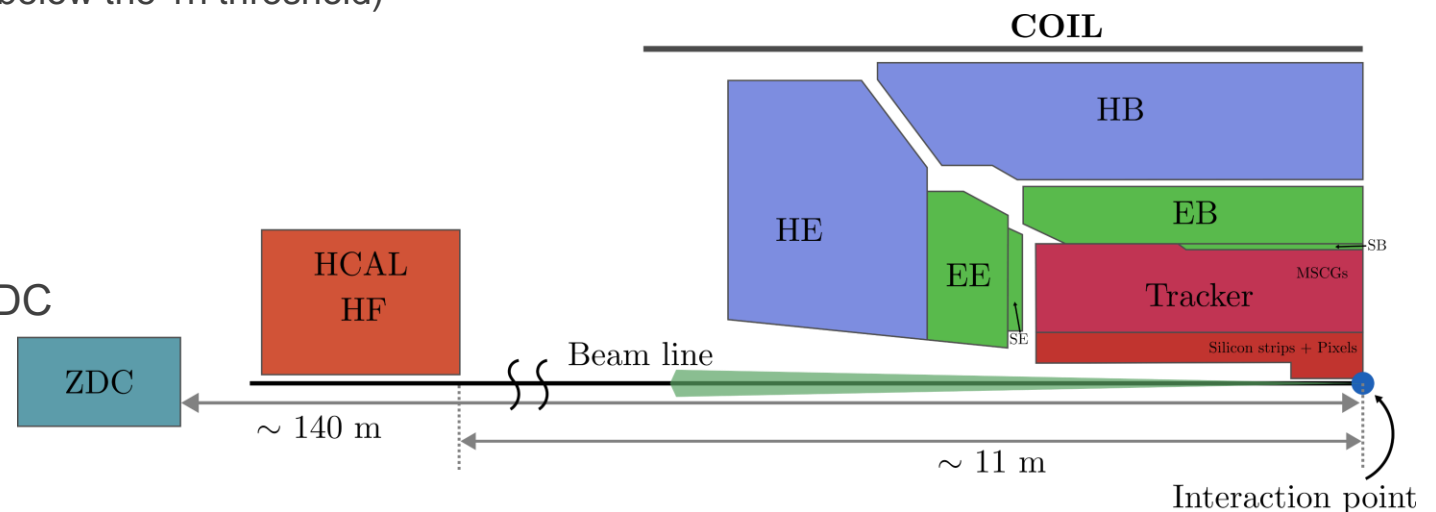
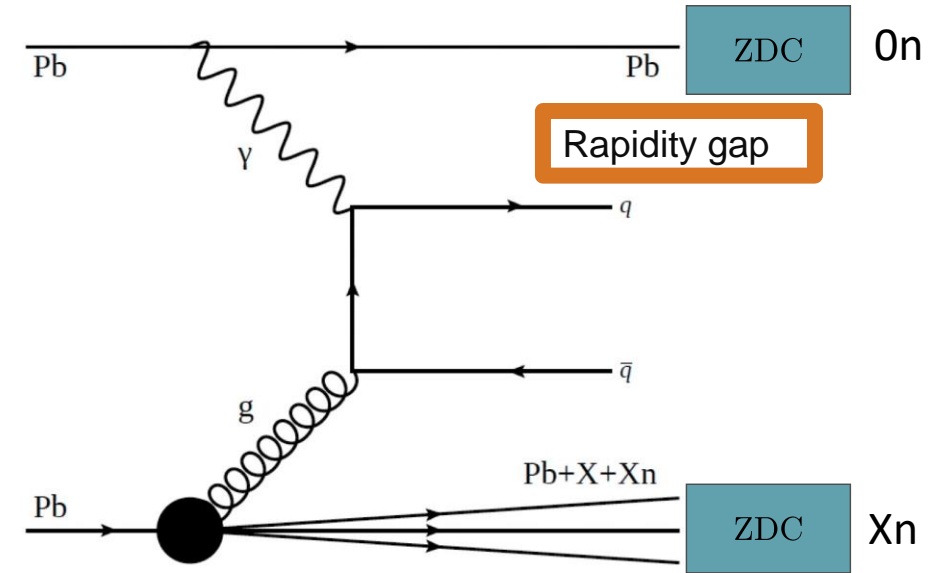
- D⁰ mesons produced in scatterings of **quasi-real photons** emitted by one nucleus with **partons** from the other colliding nucleus
- Decay channel: $D^0 \rightarrow K^- \pi^+$ (and charge conj.)

New trigger strategy for photoproduction

- New Level-1 triggers that use **both ZDC and HCAL/ECAL** information to maximize the statistics of D⁰ photonuclear events
- D⁰ p_T dependent trigger use:
 - **High p_T D⁰ → ZDC XOR** (exactly one ZDC above the 1n threshold) + **Jet trigger**
 - **Low p_T D⁰ → ZDC OR trigger** (at least one ZDC below the 1n threshold)

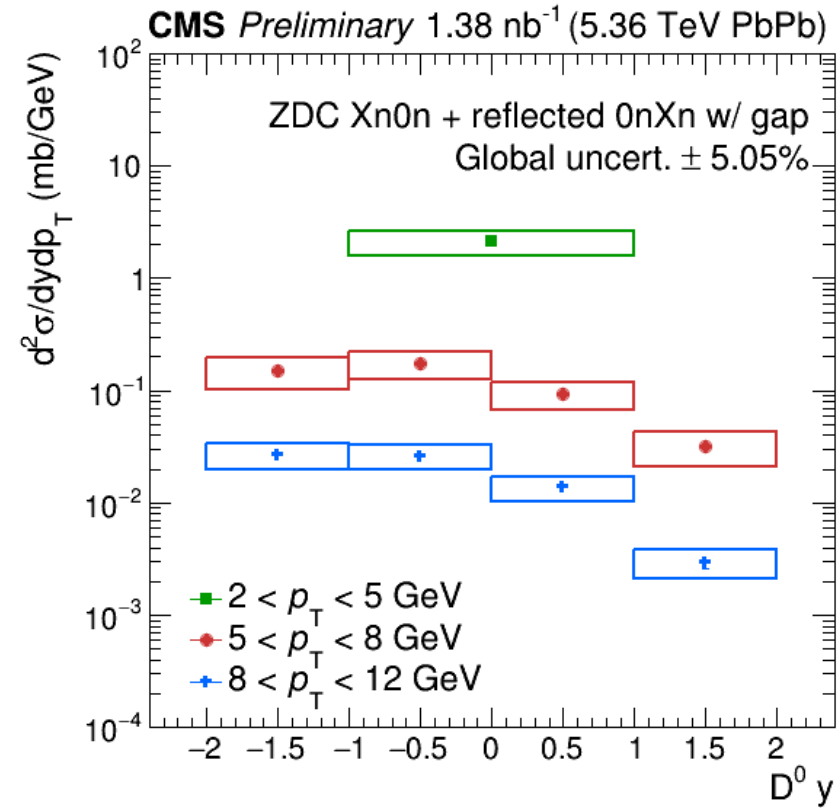
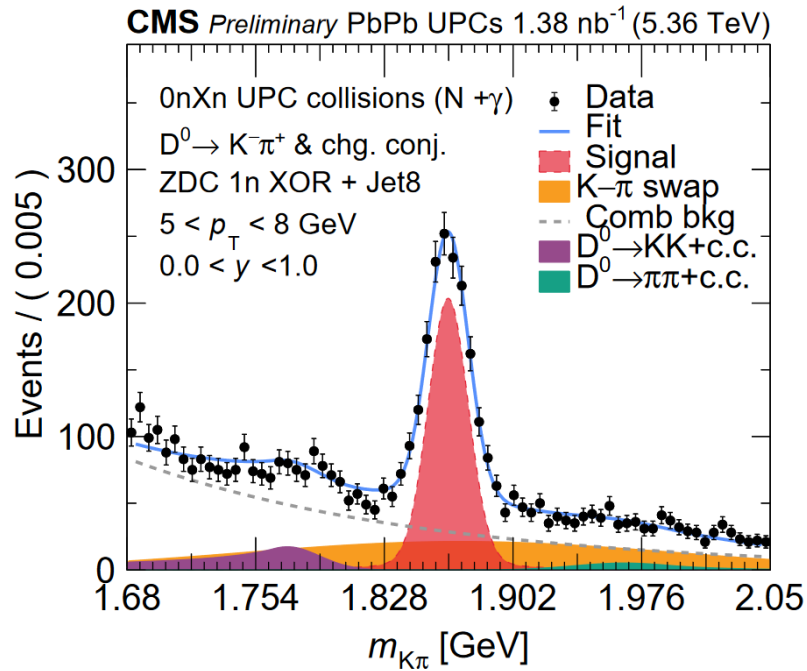
Main offline event selections

- **ZDC selection:** Xn0n or 0nXn
- **Rapidity gap** ($3 < |\eta| < 5.2$) on the side of „empty” ZDC



Final cross sections

$$\frac{d^2\sigma}{dp_T dy}(D^0 p_T, D^0 y) = \frac{1}{2} \frac{1}{\mathcal{L}\mathcal{B}} \frac{N_{D^0}^{\text{raw}}}{\epsilon_{\text{evt}} \epsilon_{\text{trigger}} P_{\text{prescale}} (\alpha \epsilon_{D^0}) \epsilon_{\text{EM,pileup}}}$$



- **Conclusions:**

- New constraints on nuclear matter with open charmed hadrons in UPCs in a large region of x and Q²
- Future: improved (x, Q²) reach with lower p_T measurements, heavy-flavour jets, correlations

Triggers for exclusive processes with photons and electrons in ultra-peripheral lead-lead collisions in the ATLAS experiment in Run 3

Karolina Domijan

AGH University + UNIBO

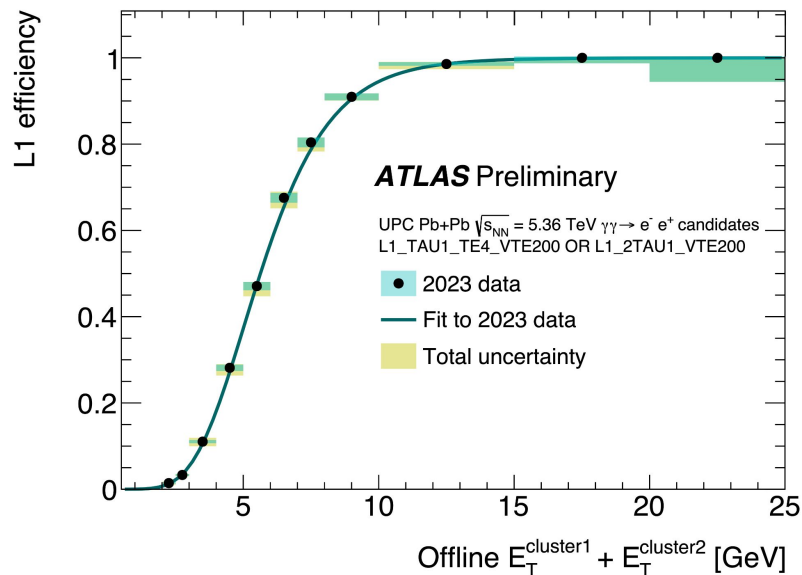


Zimanyi Winter School

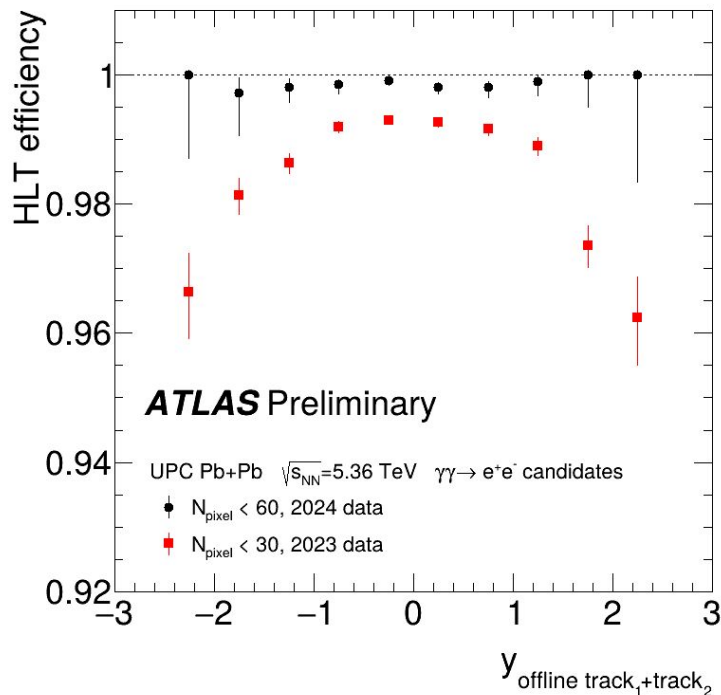
05.12.2024

L1 trigger efficiency studies

- 2023 UPC Pb+Pb data
- UPC can induce a wide variety of exclusive final states in lead–lead (Pb+Pb) collisions – dileptons, dijets, and diphotons, e.g. **light-by-light scattering**
- The performance is calculated for the log OR of two triggers, L1_TAU1_TE4_VTE200 and L1_2TAU1_VTE200, and is compared with 2018 reference data.
- The poster discusses the full performance analysis of the L1 trigger with a systematic uncertainty study



HLT trigger efficiency studies



- A comparison between **2023** and **2024** vpix trigger efficiency
- This trigger is essential for measuring photons, i.e. **light-by-light scattering**
- Veto for events with more than 30 pixel hits was introduced in Run 3 after vpix15 was deemed inefficient during the Run 2
- Veto for events with more than 60 pixel hits was introduced in 2024 in order to increase performance and reduce dependence on rapidity

CMS luminosity measurement for nucleus-nucleus collisions at 5.02 TeV

Krisztián Farkas
CMS-ELTE Lendület group
Eötvös University, Budapest

Luminosity introduction

- Determines the rate of particle collisions
- Relates the cross section of process to the observed rate

$$R(t) = \frac{dN}{dt} = L(t) \cdot \sigma_{process}$$

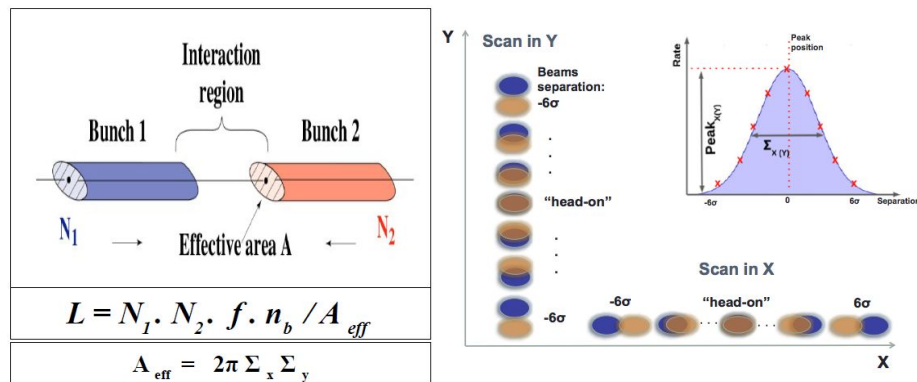
$$\sigma_{vis} = \frac{2\pi \cdot \Sigma_x \cdot \Sigma_y}{N_1 \cdot N_2 \cdot f \cdot n_b} \cdot R_{peak}$$

Why precise luminosity measurement is important?

→ Real-time feedback on accelerator performance

Luminosity measurement

- Using well-known physics process
- Using machine parameters → Beam overlap widths are obtained from vdM scan

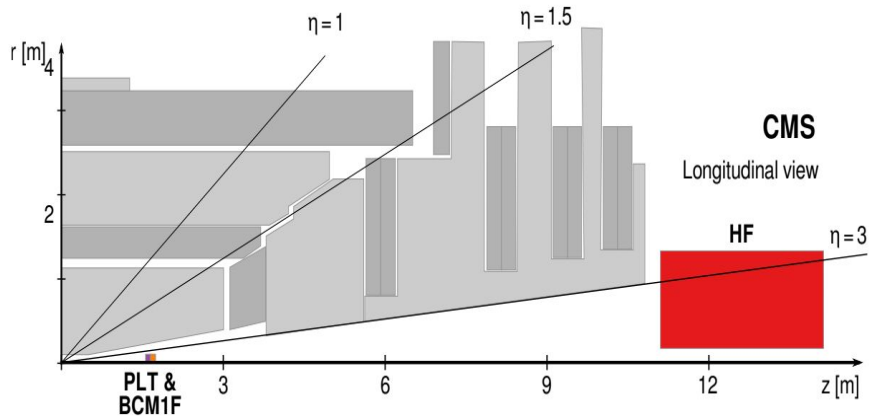


- Beams are separated in X, Y in discrete steps and measure the rate
- Various corrections applied
- Detector dependent calibration constant σ_{vis} measured then used during physics fills

CMS luminometers

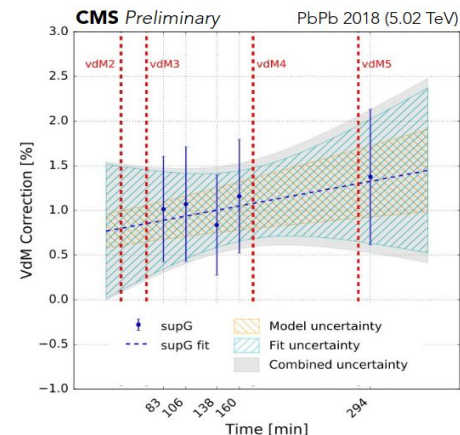
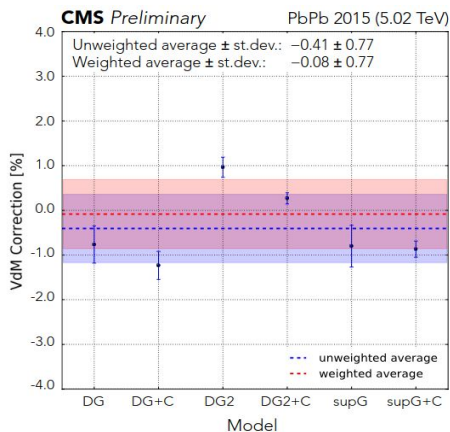
Requirement: linear measured rate-luminosity response or at least correctability

- Pixel Luminosity Telescope
- Hadron Forward calorimeters
- Fast Beam Condition Monitor
- Beam Position Monitors



Corrections to absolute luminosity

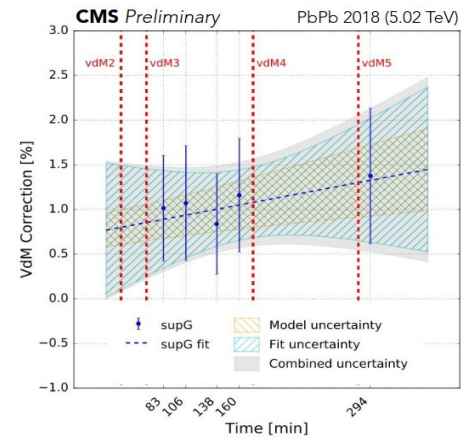
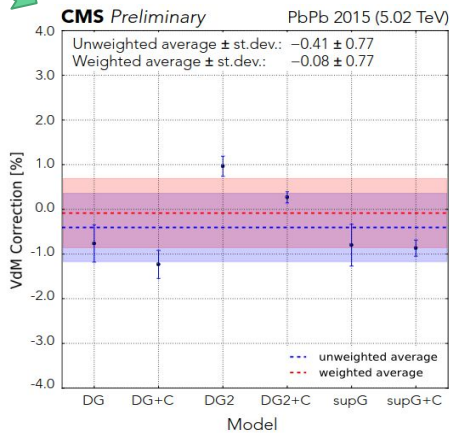
- Bunch current normalization
- Non-collision rate
- Orbit drift
- Length scale calibration
- Beam-beam effects
- Transverse factorizability



Source	2015 [%]	2018 [%]	Corr
Normalization uncertainty			
<i>Bunch population</i>			
Ghost and satellite charge	0.3	0.5	Yes
Beam current calibration	0.2	0.2	Yes
<i>Noncolliding bunches</i>			
Noncollision rate	0.5	0.2	No
<i>Beam position monitoring</i>			
Random orbit drift	0.5	0.1	No
Systematic orbit drift	0.2	0.2	Yes
<i>Beam overlap description</i>			
Length scale calibration	0.5	0.5	Yes
Beam-beam effects	0.2	0.3	Yes
Transverse factorizability	1.1	1.1	No
<i>Result consistency</i>			
Cross-detector consistency	2.5	0.4	No
Scan-to-scan variation	—	0.5	No
Statistical uncertainty	0.2	0.1	No
Integration uncertainty			
<i>Detector performance</i>			
Cross-detector stability	0.7	0.8	No
<i>Noncolliding bunches</i>			
Noncollision rate	0.1	0.1	Yes
Total normalization uncertainty	2.9	1.5	—
Total integration uncertainty	0.7	0.8	—
Total uncertainty	3.0	1.7	—

Corrections to absolute luminosity

- Bunch current normalization
- Non-collision rate
- Orbit drift
- Length scale calibration
- Beam-beam effects
- Transverse factorizability



Combined 2015+2018: 1.6% precision

Performance of the nHCal for ePIC experiment based on Simulations

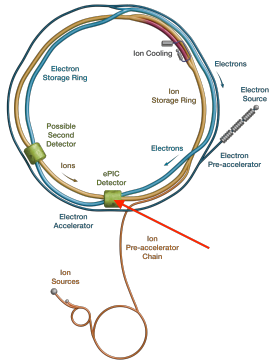
Alexander Godál

Faculty of Nuclear Sciences and Physical Engineering,
Czech Technical University in Prague

Thursday, 5 December 2024

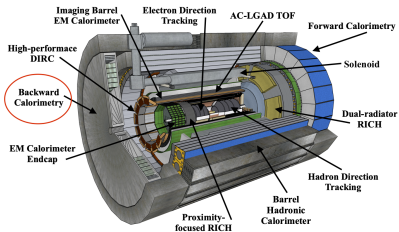


Electron-Ion Collider and ePIC detector



- approved accelerator for BNL
- repurposing a lot of infrastructure from RHIC
- both colliding beams polarised
- center-of-mass energies in the range from 20 GeV up to 140 GeV

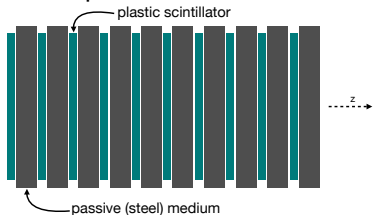
- 9.5 m long cylindrical barrel detector
- located at Interaction Point 6
- tracking and vertexing, PID, EM and hadronic calorimetry
- asymmetrical design to accommodate the difference in energies of opposing colliding beams
- large coverage in pseudorapidity



Negative Hadronic Calorimeter (nHCal) and Simulations

- sampling calorimeter in e^- direction
- tail catcher for ECal in e^- PID
- critical for ePIC \rightarrow enables precise studies at low- x

\downarrow 4 mm plastic scintillators \times 10

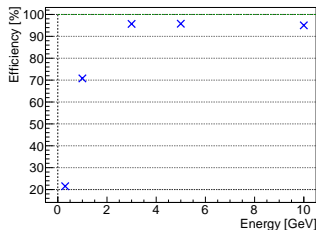


\uparrow 4 cm non-magnetic steel \times 10

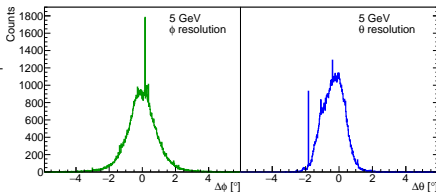
ANGULAR RESOLUTION \rightarrow

\hookrightarrow difference of reconstructed and Monte Carlo angles

RECONSTRUCTION EFFICIENCY

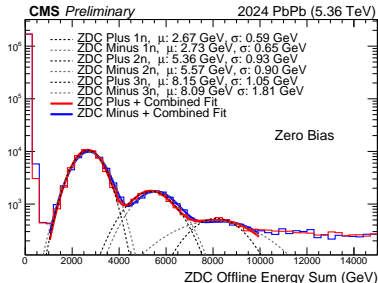
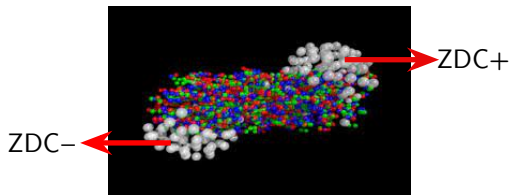
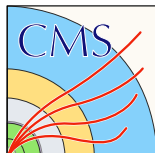


- improves with higher energies
- efficiency $> 95\%$ for $E \geq 5$ GeV



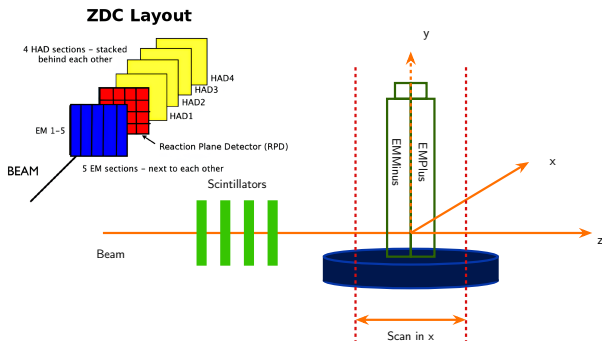
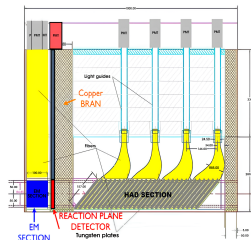
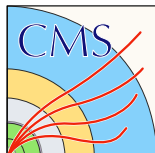
Motivation and physics behind the ZDC

- heavy-ion collisions: centrality connected to spectator neutrons
- ZDC classifies events based on neutron emission
- different neutron emission = different classes of ultra-peripheral events
- UPC: large impact parameter, no hadronic interactions
- photon-ion and photon-photon collisions



The CMS ZDC detector

- measures spectator neutrons and photons
- sampling calorimeters 140 m from CMS
- tungsten plates and quartz fibers
- EM and HAD sections: photons and neutral hadrons
- RPD: event plane for flow measurements





Eötvös Loránd University

Wigner research center for physics



ZIMÁNYI SCHOOL 2024

Poster about:

Effect of silver (Ag) doping on optical, structural, and electrical properties of SnO₂ thin films.

Prepared by a student:

Hadjra BEN HAOUA



December 5, 2024

1. INTRODUCTION/PROBLEMATIC:
Transparent Conductive Oxides (TCOs) were discovered in 1907 when German scientist Karl Rautenbach discovered a thin film of cadmium oxide (CdO). Following this, scientists and researchers became interested in creating thin-film TCOs. This is because of its applications and importance. TCOs come in two varieties, known as n-type and p-type. Indium tin oxide (ITO) and fluorine tin oxide (FTO) are well-known n-type, while copper oxides and nickel oxides are p-type. Tin oxide (SnO₂) was doped with silver in this work because it has an electron in the lattice's valence orbit, this is interesting to determine what will happen to SnO₂'s physical properties by using a cheaper method Spray Pyrolysis Technique.

2. EXPERIMENTAL WORK:
• 1. Solutions Preparation:
- Source of Tin(Sn): SnCl₄ 2H₂O
- Source of Silver(Ag): AgNO₃ dopant (0.3% Ag/Sn)
- 2:1 volume ratio of double-distilled water and methanol.
• 2. Spray Pyrolysis Technique:
Figure 1 - Photo of Spray Pyrolysis deposition system receiving inside SPFM.

3. CHARACTERIZATION TECHNIQUES:
• UV-Vis Spectrometry,
• X-Ray Diffraction,
• FT-IR Spectrometry,
• Four-Point Probe Method.

4. RESULTS AND DISCUSSION:
1. Optical properties: 1. Optical Transmission:
• Transmission is near 100% in wavelength visible light.
• The absorption region of all samples is caused by the transition between the E_{VB} and the E_{CB} is between 300 and 400 nm.
• The thickness of the sample is 400.0nm at 2.5%.
Figure 2 - Optical transmission plot of Ag (0.3 Ag/Sn%) doped SnO₂ thin films.

2. Optical Band Gap (E_g): Tauc relation:
 $(\alpha h\nu)^2 \sim h\nu - E_g$
Figure 3 - Tauc relation plots gathering the features of all samples.

5. CONCLUSION:
1) Monitoring of E_g from the first doping and its stability makes AgTO substrate AZO for tandem solar cells.
2) Most of the sample's growth is along the [110] direction.
3) The minimum value of R_{sq} is 5.93 (1/Ω) at 1.5% of Ag/Sn.
4) The maximum value of the figure of merit is 3.43x10⁻³ (Ω⁻¹) at 2.5% of Ag/Sn.

5. FOR FUTURE STUDIES:
• Use of AgTO as anti-bacterial.
• Search for gases AgTO can be widely used.
• Co-doping of Tin Oxide with Ag and Fluorine.

REFERENCES
[1] B. Benkhanou, S. Abban, A. Rahal, A. Benkhanou, M. Aida, M. S. Effect of film thickness on the structural, optical and electrical properties of SnO₂ F-doped thin films prepared by spray pyrolysis for solar cells applications, Superlattices and Microstructures, 83, (P. 88(2018)).
[2] S.M. Al, S.T. Hussain, Sh. Abu Bakar, J. Muhammad, N. Rahman, Effect of doping on the structural and optical properties of SnO₂ thin films fabricated by aerosol assisted chemical vapor deposition, Journal of Physics: Conference Series, 676, 01, 2013, (2013).

Motivation:

- Transparent Conductive Oxides (TCOs) combine two properties: conductivity, and high transparency.
- In this work, tin oxide SnO₂ was doped with silver.
- Using a cheaper method Spray Pyrolysis Technique.

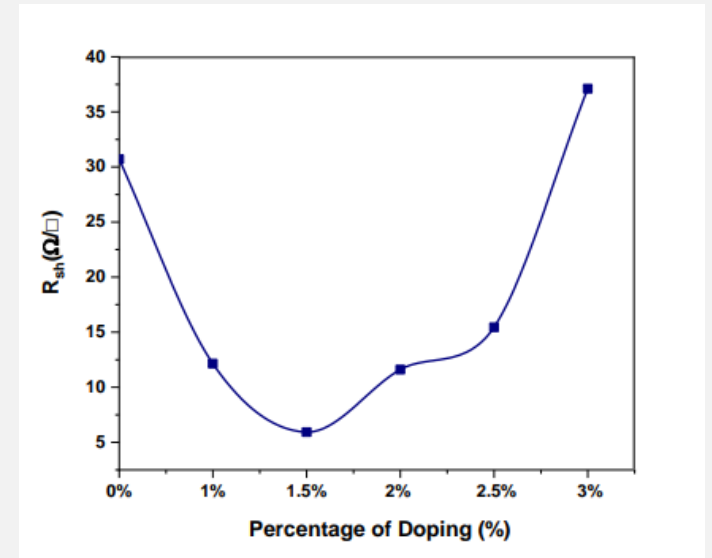


Fig.1: Draw of R_{sh} values of undoped and Ag 1-3 Ag/Sn % doped

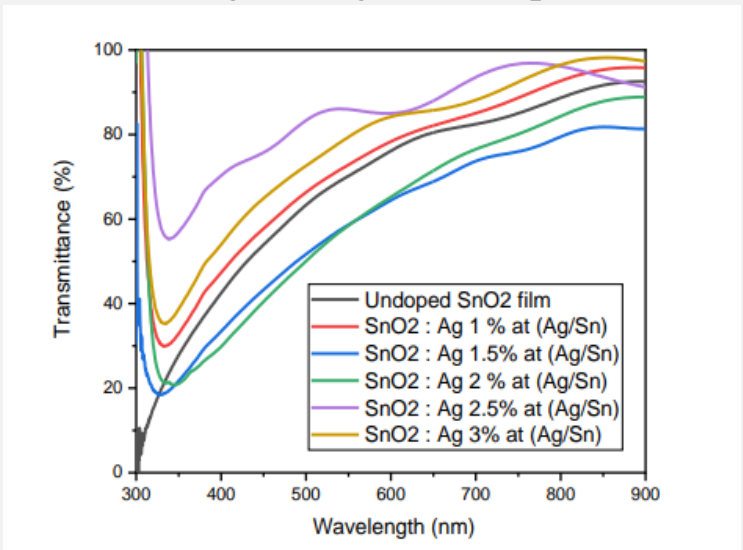


Fig. 2: Optical transmittance plot of Ag (0–3 Ag/Sn.%) doped SnO₂ thin films.

The Most Important Results:

1. Redshift of E_g from 3.76 eV to 3.07 eV.
2. The maximum value of the figure of merit is 1.427×10^{-2} (\square/Ω) at 2.5% of Ag/Sn doping.
3. Future studies will make AgTO substitute AZO for tandem solar cells.

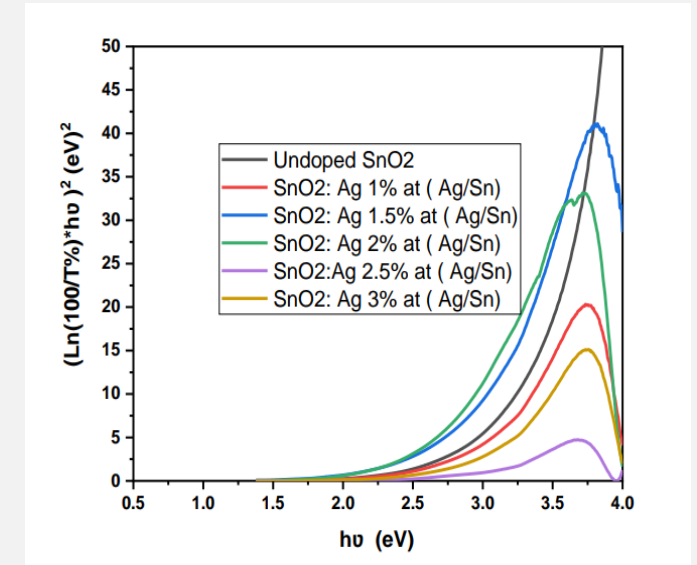


Fig. 3: Tauc relation plots gathering the features of all samples.

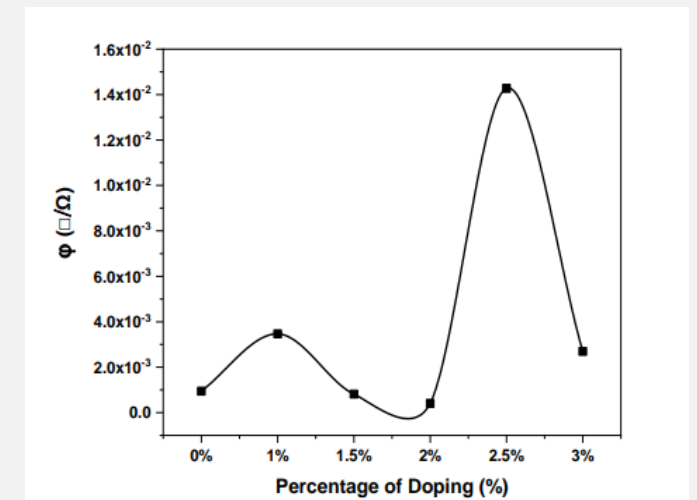
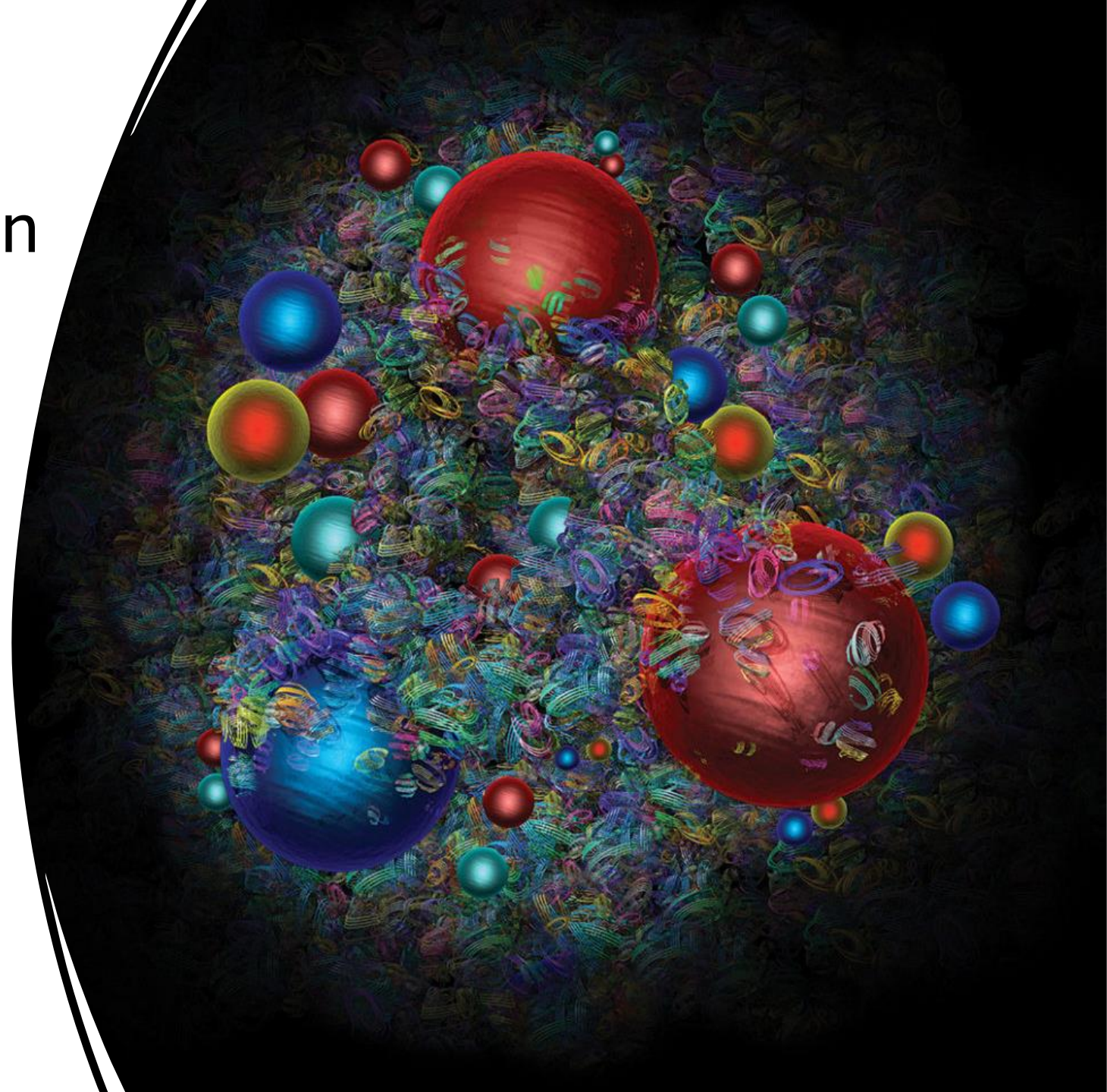


Fig. 4: Draw of R_{sh} values of undoped and Ag 1-3 Ag/Sn % doped

Quantum entanglement in high energy collisions (?)

- “The confinement of coloured quarks inside a hadrons provides perhaps the most dramatic example of quantum entanglement that exists in nature.” (Tu, Phys. Rev. Lett., 124,6)
- Can we capture the “entanglementness” of the initial partonic system?



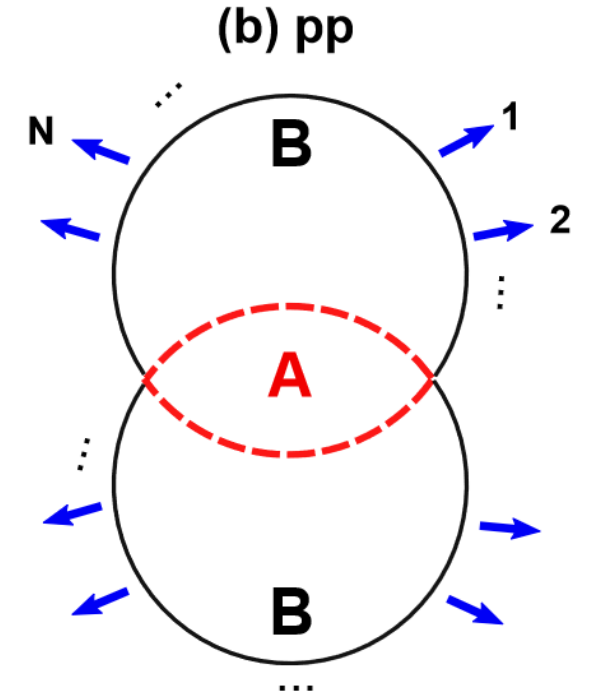
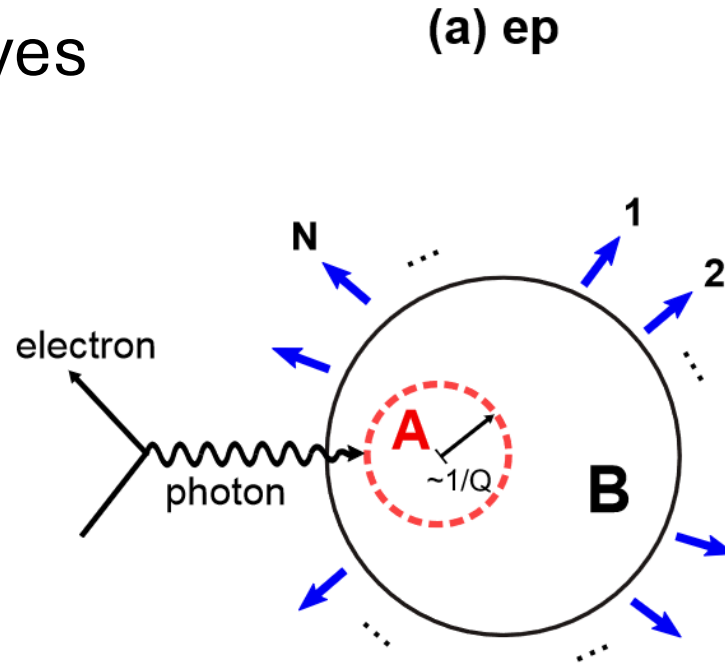
- Parton – hadron duality : yes

- Collision: sampling

- Observation: distribution of partons

- If maximally entangled, all partonic microstates have equal probability

- What is the distribution?



$$S_A = -tr[\hat{\rho}_A \ln \hat{\rho}_A] = S_B = -tr[\hat{\rho}_B \ln \hat{\rho}_B] \stackrel{?}{=} S_{\text{hadron}} = -\sum P(N) \ln P(N)$$

Maximal entanglement \Rightarrow maximal von Neumann entropy

Principle of maximal entropy \Rightarrow exponential distribution in the initial state

Parton – hadron duality \Rightarrow final state distribution: exponential distribution

Is it so? Visit my poster and find out!

Gauge field digitization in the Hamiltonian limit

Dávid Pesznyák

in collaboration with
Attila Pásztor



Eötvös Loránd
University

Zimányi School 2024
5 December 2024



HUN-REN Wigner
Research Centre for
Physics

Motivation: Complex Action Problem

partition function as a path integral

$$\mathcal{Z} = \int \mathcal{D}\phi e^{-S[\phi]} = \int \mathcal{D}\phi w[\phi]$$

if weights $w[\phi] \notin \mathbb{R}^+$ usual MCMC methods relying on importance sampling not applicable:

complex action problem

in principle, can be bypassed with the help of quantum computers

[quant-ph/1811.03629]

Digitizing gauge groups – U(1)

in the NISQ era the main bottlenecks are the limited

- circuit depths
- **number of qubits**

the Hilbert space for a gauge theory based on a continuous gauge group is infinite dimensional

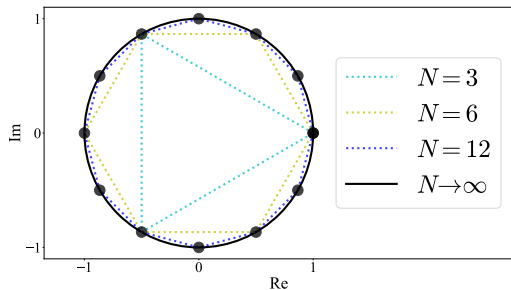


shall be made discrete and finite via **digitization scheme**

[hep-lat/1906.11213],
[hep-lat/2201.09625]

e.g. U(1) discretized to Z(N)

$$g_\infty(\varphi \in \mathbb{R}) = e^{i\varphi} \mapsto g_N(n \in \mathbb{Z}^+) = e^{2\pi i n/N}$$



DIRAC FERMIONS UNDER IMAGINARY ROTATION

Tudor Pătuleanu, Dariana Fodor, Victor Ambruș, Cosmin Crucean

West University of Timișoara

tudor.patuleanu@e-uvt.ro

4 décembre 2024



Outline of the setup

- Growing interest in studying strongly-interacting systems under rotation, usually by lattice simulations \implies SIGN PROBLEM
- Sign problem can be solved by using imaginary rotation $\Omega \mapsto i\Omega_I$.
- Present work : Free massless fermions with chemical potential μ .
- Density operator given by :

$$\hat{\rho} = \exp \left\{ -\beta \left(: \hat{H} : -\mu : \hat{Q} : -\Omega : \hat{J}_z : \right) \right\}.$$

- Thermal expectation values $\langle \hat{A} \rangle = Z^{-1} \text{Tr}(\hat{\rho}\hat{A})$ with $Z = \text{Tr}(\hat{\rho})$.

Results

- Studied t.e.v. $A_{\beta}^{i\Omega_I} \equiv \langle : \hat{A} : \rangle_{\beta}^{i\Omega_I}$ for the fermionic condensate $\bar{\Psi}\Psi$, the currents J_V, J_A, J_H and the energy-momentum tensor T .
- Interesting behavior in systems undergoing imaginary rotation : FRACTALIZATION far away from the rotation axis. This is defined as a $1/q^n$ dependence for rational values and 0 for irrational values.
- The chemical potential term breaks fractalization (it is q -independent).
- Consequence : there is no analytic continuation to real rotation, outside of the rotation axis.

Anomalous $U(1)_A$ couplings and the Columbia plot

Péter Kovács, Győző Kovács

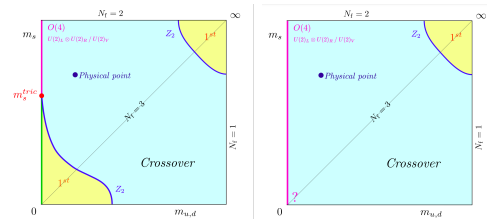
HUN-REN Wigner RCP

Zimányi 2024 Falsh Talk session
2-6 Dec 2024

Collaborators: Francesco Giacosa, Győző Kovács, Robert D. Pisarski, Fabian Rennecke



Columbia plot scenarios



F. Cuteri, O. Philipsen,
A. Sciarra, JHEP 11
(2021) 141

We tested whether these different behaviors could be caused by different $U(1)_A$ terms.

